R. & M. No. 3437

MINISTRY OF AVIATION

AERONAUTICAL RESEARCH COUNCIL
REPORTS AND MEMORANDA

The N.P.L. 59 in.×9 in. Boundary-Layer Tunnel

By P. Bradshaw and G. E. Hellens

LONDON: HER MAJESTY'S STATIONERY OFFICE
1966
PRICE 13*s*. 6*d*. NET

The N.P.L. 59 in.×9 in. Boundary-Layer Tunnel

By P. Bradshaw and G. E. Hellens

*Reports and Memoranda No. 3437**

October, 1964

Summary.

A description is given of the tunnel, which is of the closed-circuit type, with a top speed of 150 ft/sec and a 10 ft long working section, with a flexible roof to impose any desired pressure gradient on the floor boundary layer on which the measurements are made. Results are given of a complete calibration of the working section and return circuit. Full details of the construction are given in an Appendix.

1. *Introduction.*

The tunnel was designed for the study of two-dimensional boundary layers, especially turbulent layers, in controllable pressure gradients. It seemed to be essential, in any systematic study of turbulent boundary layers, to establish pressure gradients which had a meaning in terms of the properties of the boundary layer itself: a great deal of generality is lost by doing experiments on boundary layers on arbitrarily chosen aerofoils or in ducts of simple geometrical shape. The original idea was to do experiments in a conventional wind tunnel but mechanical convenience made a flat working surface preferable, and after consideration and rejection of a duct, with one flexible wall, hung in a tunnel working section, it was decided to design a complete small wind tunnel and thus avoid occupying an unnecessarily large wind tunnel for long periods.

Space limitations and power economy, and the desirability of imposing the required pressure gradient on a flat working surface by deforming the opposite wall of the tunnel, led to the choice of a shallow working section. A Reynolds number Ux/ν of about 10^7 was regarded as necessary and in view of the interest at that time (1958) in surface shear-stress measurements a nominal speed of 150 ft/sec was chosen to give a shear stress high enough to measure comfortably. The length of working section required was thus about 10 ft. A slower speed and a longer working section would have produced thicker boundary layers and made hot-wire measurements near the surface easier but the overall size of the tunnel would have become excessive. A working-section width of 5 ft† was chosen in the hope of maintaining nearly two-dimensional flow, without noticeable convergence due to growth of boundary layers on the sidewalls, in fairly strong adverse pressure gradients: it was realised that studies of separating layers were likely to be impracticable in general. The nominal height of the working section was chosen as 9 in. to give an adequate region of potential flow between the floor and roof boundary layers (the total thickness of the floor boundary layer in zero pressure

* Replaces N.P.L. Aero. Report No. 1119—A.R.C. 26 296. Published with the permission of the Director, National Physical Laboratory.

† (later reduced to 59 in. so that 5 ft wide standard sheets of plywood could be used).

gradient would reach about 2 in. at the end of the working section: the greater thickness of retarded boundary layers would be compensated by the increased roof height required to produce the adverse pressure gradient).

It was decided to make this a *closed-circuit* tunnel. The extra complication was accepted because (i) as the tunnel was to be used for hot-wire measurements, clean air was held to be essential, and the possibility of filtering 35 000 c.f.m. of London suburban air to remove all particles down to sub-micron size (a typical wire diameter being 0·0002 in. or 5 microns) was regarded as remote, (ii) a power factor of 0·5 or better could be expected with a closed-circuit tunnel whereas that of an open-circuit tunnel of the type used by Clauser[1] would probably approach 2: it was intended at the time to use the tunnel for extensive work on transition as well as turbulent boundary layers and it was therefore desired to minimise turbulence, and vibration and noise from the motor and fan. This was an additional reason for rejecting Clauser's arrangement in which the pressure gradient was controlled by blowing large quantities of air through the roof into the atmosphere. The positive advantages of a closed-circuit tunnel were that suction on the working-section walls could be applied merely by blowing air into the tunnel elsewhere, whereas overpressure in an open-circuit tunnel working section could only be achieved with a power factor greater than unity; and that the air in the tunnel could be kept clean if clean air were continuously blown in so that any dust should eventually be blown out.

Suction on the working-section walls was required to keep the boundary layer on the (curved) roof attached when the boundary layer on the (flat) floor approached separation, and to prevent separation, or excessive boundary-layer growth, in the corners. The obvious way of replacing the air was by tangential blowing at the entry to the first diffuser, as it was considered improbable that a diffuser with such thick boundary layers at entry would function efficiently without it, particularly as the cross-section was to change from a 59 in. × 9 in. rectangle at the end of the working section to a circle at the fan (in fact the cross-section becomes a regular octagon by the first corner).

Because the working section was rather long ($4\frac{1}{2}$ equivalent diameters or 30 hydraulic mean depths) and because it would have been unwise to make the first diffuser short, the settling chamber and contraction had to be kept as short as possible, to minimise the overall length of the tunnel. It was convenient to use a two-dimensional contraction, permitting an area ratio of about 12 with a working-section floor 5 ft above the floor of the room, and also permitting exact design by the method of Ref. 8.

The remainder of the tunnel is conventional, and the general design follows the principles stated in Ref. 2 (that paper includes photographs of the fan assembly): contrariwise the latter paper incorporates the fruits of experience with the boundary-layer tunnel.

The basic design dates from early 1958: detailed design commenced in the autumn of that year. The tunnel first ran in May, 1961 with a temporary plywood working section, and the flexible-roof working section was finally completed in July, 1963.

This report begins with a description of the tunnel circuit, including a discussion of the modifications made during commissioning: then the flow in the tunnel in its final state is described. An Appendix to the report gives details of the structural design.

No apology is offered for producing such a large report on such a small tunnel: if tunnel design is to progress, information must be made available on the performance of existing tunnels, especially those with special features, but, at present, comprehensive low-speed tunnel calibration reports could almost be counted on the fingers of one hand.

The Working Section.

The boundary layer on the lower surface of the contraction is bled off at the start of the working section (Fig. 2) so that the test boundary layer has its origin at the leading edge. The leading edge is sharp, with a 12° chamfer on the lower surface (Fig. 5b). The Perspex side walls have $\frac{1}{8}$ in. slots every 2 in., with a $\frac{1}{4}$ in. radius on the upstream and downstream sides. The roof is made up of slats, also with $\frac{1}{8}$ in. (nominal) gaps between them (Fig. 2) but at present with a radius on the downstream side of the slot only: the divergence on the atmosphere side of the $\frac{1}{8}$ in. throat is primarily intended to prevent the gaps closing when the roof is convex downwards, but there may be some static-pressure recovery when suction is being applied. The roof suction is controlled by slide valves on top of the slats. The slats are threaded on to two longitudinal steel strips to preserve a smooth curve, and every other slat is adjusted by means of jacking screws to give the desired roof shape: the slats slide up and down in the $\frac{1}{8}$ in. slots in the side walls.

The alternative roof arrangement would have been a uniformly porous surface, like that used on the N.A.S.A. Lewis boundary-layer channel[3]. The slat arrangement was preferred for structural reasons, partly because of the desire to set quite sharp bends in the roof, but the boundary layer on this rather peculiar surface grows at about 1·7 times the rate of a boundary layer on a smooth surface. Originally, the slots had radii on both the upstream and downstream sides in order to minimise the effect of sudden changes in roof slope from one slat to the next. A 9 in. span, 30 in. chord mock-up was tested in the vertical wall of the temporary working section to verify that the boundary layer was well behaved: in fact the rate of growth was only about 10% greater than that of a boundary layer on a smooth surface. However, when the roof was completed it was found that the roof boundary layer near the rear of the working section was about three times the theoretical thickness and oscillated, randomly but with an average frequency of about two cycles/sec, between a 'thin' and a 'thick' state. The pressure in the plenum chamber between adjacent slats was higher than in the free stream by about 0·1 of the dynamic pressure, indicating that the boundary layer was remaining attached round part of the slot entry radius and intermittently discharging air into the plenum chamber. The trouble was cured by glueing capping pieces to the slats to provide a sharp edge to the slot entry (Fig. 12). The boundary layer was still considerably thicker than on a smooth surface, contrary to what was indicated by the tests of the mock-up: in view of the pronounced secondary flow subsequently found near the vertical wall it may be conjectured that the flow over the mock-up was not two-dimensional. The flow near the walls is steady and the wall slots have not been modified.

It was originally intended to set the slat positions by hand-driven jacks and to adjust the roof suction by taping over the outside of the slots, but it became apparent during detail design that, for rigidity and freedom from vibration, the slats would have to be about 2 in. thick (wood) and therefore rather heavy to jack by hand. When a motor-driven scheme was considered it was decided further to reduce the labour of setting the roof by having proper control valves for the suction slots: the sidewall slots are blocked when necessary by T-section plastic strip, manufactured commercially for the embellishment of home-made furniture. These changes from the original design have greatly increased the versatility of the tunnel, and the roof can be completely re-set in a matter of a few minutes, but the changes were partly responsible for the considerable delays in construction of the tunnel.

The roof height can be adjusted continuously between 5 and 14 in. except at the front and rear where the height is necessarily about 9 in. The maximum change of slope between adjacent slats

is about 25°: it is of course impossible to impose *discontinuities* of pressure or pressure gradient on a flat surface by means of a curved liner and if the increment in roof slope were made much larger it would be impossible to prevent separation of the roof boundary layer even with the aid of boundary-layer suction.

For tests in power-law adverse pressure gradients ($U_1 \propto x^{-a}$) a fairing, 21 in. chord and 1·6 in. thick, is attached to the leading edge and the front floor plate: this enables much higher velocities to be obtained near the origin of the boundary layer. A specimen pressure distribution and the corresponding roof settings are shown in Figs. 1 and 2 of Ref. 18.

The six floor plates, each 18 in. in (streamwise) length, have $3\frac{1}{2}$ in. diameter holes into which instrument-carrying discs are inserted, giving a line of measuring stations every 6 in. down the centre line, with additional stations at ± 6 in. from the centre line at 18 in. streamwise intervals. To permit continuous spanwise coverage, any floor plate can be slid sideways by ± 9 in. by means of a hand-driven jack temporarily bolted between the floor plate and the working-section frame. This last facility has proved very useful for rapid checks on two-dimensionality, although it led to the additional structural difficulty that the side walls had to be cantilevered from the overhead frame instead of being attached directly to the floor plates.

The use of plug-in discs with instruments permanently attached to them was inherited from the work of Ref. 4 in which Stanton tubes and Preston tubes were mounted on $3\frac{1}{2}$ in. discs so that they could be transferred from a flat plate to a duct: this arrangement has great advantages because traverse gear can be set up, or pressure transducers aligned flush with the surface, before insertion in the tunnel. Empty discs carry pressure tappings, so that the static pressure can be measured at intervals of 3 in. or less down the centre line of the tunnel. These pressure tappings, and the various other pressure tappings in the tunnel, are connected to the 144 inputs of a pressure switch, operating by pinching tubes, by means of which 36 pressures at a time can be fed to a multi-tube inclined manometer. The manometer angle can be adjusted to set the reference pressure difference (measured across static-pressure tappings in the contraction) to 10 in. of liquid so that pressure coefficients can be read off directly. In normal operation of the tunnel the pressure gradient is fixed over a long series of runs and does not have to be recorded at frequent intervals, so that a single manometer and a pressure switch were preferable to a large bank of manometers or a pressure transducer and 144-port scanning valve.

At the downstream end of the working section, 0·08 in. high tangential blowing slots (Fig. 5a) are provided on the roof and floor. The jets blow over $\frac{1}{2}$ in. wide breathers and entrain atmospheric air like an induction pump, so as to minimise the consumption of high-pressure air, which is supplied from the 350 p.s.i. storage bottles *via* a porous-disc pressure reducer. The quantity entrained is about 50% of the primary jet flow for zero pressure difference between working section and atmosphere. Impregnated cloth filters are fitted over the breathers, and all the accessible parts of the return circuit, including the second and third corners, the fan assembly, the second diffuser and the contraction, and the approaches to the hatchways, are coated with Takdust gel, a dust-absorbent compound that is more effective and much less offensive than grease. A further jet is provided at the tail of the fan nacelle and can be used if the quantity of air required for the roof suction greatly exceeds the blowing quantity required to give fully attached and roughly axisymmetric flow in the first diffuser.

The First Diffuser.

The cross-section changes from a 59 in. × 9 in. rectangle at entry to a regular octagon, 33·3 in. across the flats, at the first corner (area ratio 1·73): the equivalent cone angle is about 5°, which was

considered to be the maximum permissible in combination with such a rapid change of cross-sectional shape, even with the aid of boundary-layer control. Static-pressure tappings, and rod-type pitot tubes with the holes 2 in. from the surface, are fitted on the top, bottom and vertical sides just ahead of the first corner section, and are used to check that the flow is fully attached. The bulb of a remote-reading mercury-in-steel thermometer is fitted near the floor at the entrance to the diffuser to record the temperature of the air in the working section before it mixes with the colder air from the blowing slots: the indicating dial is mounted near the control panel.

Diffusion continues, at approximately 5° equivalent cone angle but without further change of cross-sectional shape, between the first and second corners. The area ratio at the second corner is 2·25, the distance across the flats of the hexagon being 37·9 in.

The Corners.

All four corners have 10½ in. chord vanes of circular-arc section, with 1in. long straight extensions at leading and trailing edges for ease of construction. The subtended angle is 86°, the trailing edge being set parallel to the centre line of the tunnel. The spacing is about 2·5 in., adjusted so that all the gaps in a given corner are equal. The performance of the corners has been entirely satisfactory.

The Fan Section.

The 8-bladed fan is driven by a 15 h.p. 600 r.p.m. d.c. shunt wound electric motor supplied from a grid-controlled mercury arc rectifier (Messrs. Lancashire Dynamo Nevelin 'Varionic' drive). The rectifier is controlled through a pilot motor, operated remotely from the tunnel control panel. A motor vehicle propeller shaft, 3 in. in diameter, connects the motor to the fan. The shaft is faired where it is not parallel to the airstream; without the fairing, the power factor rose by 0·03.

The fan was designed to absorb 12 h.p. at 600 r.p.m. at a mean axial speed of 67 ft/sec. The diameter is 48·4 in. ($U/\Omega D = 2{\cdot}64$), the nacelle diameter 30 in. ($0{\cdot}6D$) and the blade chord 11·25 in. The blade section is 10% Clark Y and the blade angle decreases from 47° at the root to 32·7° at the tip ($0{\cdot}9 > C_L > 0{\cdot}7$). The design method[2] was basically the isolated-aerofoil method described by Mair[5] in which the lift coefficient at each radius is calculated from momentum considerations and the angle of incidence of the chosen aerofoil section obtained from data relating to the same aerofoil in an infinite stream, semi-empirical corrections being made for the effect of blade interference on the lift slope and no-lift angle near the roots where the gap/chord ratio is small. This method appears better suited to the design of moderately loaded fans than the 'camber-line' method used for multi-stage axial compressors, because the empirical relations on which the latter method is based become unreliable at the larger gap/chord ratios near the tips of the blades. The 15 pre-rotation vanes were also designed by Mair's method, using NACA 6712 aerofoil section, although the gap/chord ratio was everywhere low enough for the camber-line method to be used. The pre-rotation vane trailing edges were made adjustable but have not so far been touched. Nine uncambered, undeflected straightener vanes, inversely tapered to give a gap/chord ratio of unity, are installed downstream of the fan.

The cross-sectional area remains very nearly constant up to the fan as the cross-sectional shape changes from octagonal through hexadecagonal to circular, and increases slightly over the rear of the fan nacelle as the cross-sectional shape returns to octagonal. The fan nacelle tail is fitted with an air jet, actually consisting of a 3 in. disc, drilled with 37 ¼ in. diameter holes, supporting a porous-metal pressure reducer: the base can be covered by a conical fairing when the air jet is not in use.

Speed Control Gear.

The pilot motor which drives the potentiometer controlling the rectifier grid voltage is incorporated in a quasi-proportional control system using a pair of silicon controlled rectifiers to supply the pilot-motor armature with a voltage depending on the error signal of a pressure transducer: the system is similar to that described by Johnson in Ref. 6, but certain complications are introduced by the need to retain the safety interlocks in the manual control system, and to make the system proof against mishandling, power supply failure, etc.

The pressure transducer used is a liquid manometer with a lamp and photocell arranged on opposite sides of one limb and enclosed in a light-tight box. The photocell is of the photoconductive type and is used in an a.c.-excited Wheatstone's bridge. The photocell resistance varies roughly linearly over the small range of meniscus position commonly experienced. The advantage of this type of pressure transducer is that its sensitivity is limited only by the sensitivity of an inclined-tube manometer: it is quite possible to obtain a magnification of 25 by inclining the manometer tube, so that the tunnel can be controlled at low dynamic pressures where the mechanical hysteresis of diaphragm-type gauges would be excessive. A small manometer has been made specially, with a fixed sight tube and photocell unit and a reservoir which is moved up and down a rack by a hand-wheel: the rack is engraved with a scale of inches. Unfortunately, the system is not able to compensate immediately for sudden fluctuations in mains voltage and it does not seem possible to combine *speed* control and *voltage* control except by fitting voltage stabilizers in each phase of the rectifier supply.

Second Diffuser.

After the end of the fan section the cross-section shape changes from octagonal to square in a length of 66 in. or 1·6 times the initial equivalent diameter. The expansion continues at approximately 5° equivalent cone angle to an area ratio of 6·56 (59 in. square) just before the third corner. The reason for using a square section is to simplify construction, particularly of the corner vanes. The cross-section remains square and of constant area from the start of the third corner section to the start of the wide-angle diffuser.

The Rapid Expansion.

The height of the tunnel increases from 59 in. to 107 in. in a distance of 29½ in. (wall angle 35°). The corners at the beginning of the expansion are sharp but the concave corners at the end are faired. There are two screens, of 30 mesh, 34 s.w.g. (0·009 in. diameter) wire: the pressure-drop coefficient of the screens is about 2 for speeds corresponding to nearly full speed in the working section.

Settling Chamber.

The settling chamber contains a honeycomb with 4 in. long right-angled triangular cells having a hypotenuse of 2 in., and four screens. Originally the honeycomb was fitted immediately downstream of the wide-angle diffuser but when the tunnel was moved from one building to another in 1962 the opportunity was taken to replace the honeycomb 6 in. downstream to give the flow a chance to become more nearly parallel to the axis before entering the honeycomb so that the cells near the roof and floor should run full. The r.m.s. turbulence level downstream of the last screen previously rose, near the floor, to about 1·5 times the value near the centre line: this increase was almost eliminated by the modification, although the turbulence level in the working section was satisfactory in any case and the modification was more cosmetic than essential.

Originally, three 30 mesh 0·009 in. screens were fitted, each in a wooden frame which also formed the shell of the tunnel. These screens had been badly wrinkled by careless storage and a fourth screen of 20 mesh, 0·0148 in. wire was added later. In order to minimise the tension in the wires the intersection between a screen and its frame was arranged to lie on a sphere: however, this attempt to persuade a flat screen into a curved surface was not really successful and even the fourth screen had wrinkles. It was found that the boundary layer in the working section exhibited spanwise variations of surface shear stress of up to $\pm 10\%$ of the mean, an effect also found by other workers (although it does not seem to be present in all tunnels: if the V-component fluctuations in the settling chamber are large, the pattern will be smoothed out). At that time it was thought that the wrinkles were entirely to blame, so the worst of the 30 mesh screens was removed and two more 20 mesh screens were added, clamped flat between pairs of frames and admirably free from wrinkles. However, the surface shear-stress variations persisted and were subsequently traced[7] to an instability in the flow through the screens. Tests of a range of screens in a smaller test rig showed that spanwise variations occurred downstream of all screens with open-area ratios of less than about 0·57: similar effects can be caused by wrinkles, since the shear-stress variations appear to be produced by variations in flow direction. It was found that the boundary-layer profiles at different spanwise positions were of different shape as well as different thickness, and therefore could not be typical of a two-dimensional boundary layer.

Finally, four 16 mesh, 0·0148 in. screens (open-area ratio 0·58) were fitted, two curved and two flat, in the positions shown in Fig. 1. The surface-friction variations were then reduced to less than $\pm 3\%$, attributable to the remaining wrinkles in the screens and non-uniformity of the honeycomb.

Contraction.

As mentioned above, it was expedient to use a two-dimensional contraction so that it could be designed exactly and thus made as short as possible. Lighthill's[8] method was used: the wall slope χ and the logarithm of the velocity q on the wall are conjugate functions of the angular co-ordinate on a circle from which the contraction is conformally transformed. The velocity was chosen as

$$\log_{10} q = -0{\cdot}53959\ (\cos\theta + 0{\cdot}8\sin^2\theta),$$

giving

$$\chi\ (\text{deg}) = 71{\cdot}187\sin\theta\ (1 - 0{\cdot}8\cos\theta).$$

An element of arc on the contraction wall is

$$ds = \frac{d\theta}{q\sin\theta}$$

from which the co-ordinates of each point can be obtained by integrations. Unfortunately it is not possible to choose q directly as an algebraic function of s.

The resulting contraction shape is shown in Fig. 1 and the ordinates are given in Table 1. The contraction is truncated at $\theta = 7°$, $\chi = 1{\cdot}7°$ by the last screen frame. This is actually the second contraction to be designed: the first was a more exaggerated version with a maximum wall angle of 92°, and calculation showed that laminar boundary-layer separation might just occur in the *wide* end. A 1/9 scale model of the present contraction was built to satisfy non-mathematical objections, and performed satisfactorily except that Taylor-Görtler instability occurred on the concave surface. As it was anticipated that transition to turbulence would occur at full scale by virtue of the adverse pressure gradient alone, the design was accepted.

Unfortunately it was found that the turbulent boundary layer on the full-scale contraction did not revert completely to the laminar state on passing through the region of strongly favourable pressure gradient. According to Preston[9] a fully developed turbulent boundary layer cannot exist at Reynolds numbers $U_1\delta_2/\nu$ less than about 320, but decay of the turbulence will clearly take many boundary-layer thicknesses after the Reynolds number has fallen to this value. Theoretically, the Reynolds number $U_1\delta_2/\nu$ will be reduced, by a contraction so sudden that the effect of surface shear stresses can be neglected, in the ratio $c^{-(H+1)}$ where c is the contraction ratio and H is the shape parameter of the boundary layer, assumed constant. H is necessarily greater than 1 so that c^{-2} can be taken as a conservative ratio. In the present case $U_1\delta_2/\nu$ is roughly 1500 before the sudden contraction so that it should fall to 10 after it: however the profile would be far from the zero-pressure gradient shape considered by Preston, and the growth of the boundary layer due to surface shear stress is considerable. Perhaps a longer, less violent region of favourable pressure gradient would be preferable for wind-tunnel contractions. At all events, the boundary layer at the narrow end of the contraction is transitional at the higher tunnel speeds (Fig. 20) and its displacement thickness fluctuates so that there are still appreciable (inviscid) velocity fluctuations at $\frac{1}{4}$ in. ($2\frac{1}{2}$ boundary-layer thicknesses) above the surface, the height of the leading edge. The resultant intermittent adverse pressure gradients in the fresh boundary layer formed on the working-section floor caused transition to turbulence at quite low Reynolds numbers. Although a turbulent boundary layer is required for most of the work in the tunnel, and in fact many other investigators, including Clauser, appear not to have bled the contraction boundary layer away at all, it seemed advisable to check that the fluctuations near the leading edge (which, being inviscid, are bound to die away downstream) did not affect the development of a turbulent boundary layer downstream of a trip wire. Accordingly, rows of holes were drilled in the contraction floor near the point of maximum wall angle, allowing air to be sucked from the boundary layer by the overpressure in the tunnel, until the boundary layer under the leading edge became laminar. It was found that the mean-velocity profile in the boundary layer at $x = 22$ in. was the same, to within the accuracy of measurement, both with and without suction in the contraction. (This is not an absolute guarantee that the similarity extends to the details of the turbulence structure but further checks can easily be made as required.) Therefore, the tunnel is normally run with the holes in the contraction taped over to minimise the injection quantity: a laminar boundary layer can be obtained for tests on transition (Tollmien-Schlichting waves were observed incidentally during the course of the explorations mentioned above) or for checks on the freedom of pressure transducers from vibration simply by removing the tape and the trip wire.

Working-Section Calibration.

Thanks to the refined screen arrangement, the small-scale spatial velocity variations at the front of the working section are too small to measure. Traverses with a hot wire in the settling chamber showed that the velocity there varied by not more than $\pm\frac{1}{2}\%$, compared with about $\pm 2\%$ behind the old screens, and this figure probably represents an upper bound because the tests were made with a strong adverse pressure gradient in the working section and no tangential blowing, so that the tunnel speed was slightly unsteady. The velocity variations in the working section may be assumed to be $\pm\frac{1}{2} \times (1/12)^2 = 0{\cdot}003\%$ or $\pm$ 0·06 in./sec in 150 ft/sec: this implies about $0{\cdot}001\%$ *r.m.s.* variation, so that the spatial variations are much smaller than the turbulent fluctuations.

The turbulence intensity and spectra near the front of the working section, measured with the apparatus described in Ref. 10, are shown in Figs. 10 and 11. Earlier measurements, taken when the tunnel was installed in a room which it very nearly filled, showed that the u-component 'turbulence' level at the lower speeds was noticeably affected by the atmospheric wind: on a very windy day, the turbulence level was roughly independent of tunnel speed. Also, rapidly opening and shutting the large double doors at one end of the room produced noticeable surges in tunnel speed. There is no reason to think that this tunnel is particularly sensitive to draughts, and similar results would probably be obtained in other low-turbulence tunnels. The fluctuations are, of course, too low in frequency to affect transition directly, but might be important in tunnels used for tests on oscillating models. The u-component intensity in these early measurements, made with the old, 'supercritical' screens, was the same as that shown in Fig. 10, within the experimental accuracy: the lower cutoff frequency of the apparatus used for the early measurements was about 3 c/s compared with 2 c/s in the case of the later results. Certain other modifications had been made to the tunnel between the two sets of measurements (including the re-siting of the honeycomb) so that the conclusion is that replacing four screens of open-area ratio 0·5 by four screens of open-area ratio 0·58 does not significantly increase tunnel turbulence.

The u-component fluctuation consists almost entirely of low-frequency surgings and unsteadiness: about one-third of the energy is contained in wavelengths longer than the working section. The low-frequency contribution is reduced by applying tangential blowing in the first diffuser, but there was no noticeable *increase* when an obstacle roughly 18 in. high and 5 ft. wide (the senior author) was placed on the floor of the second diffuser just upstream of the third corner: therefore, unsteady separations in the high-velocity part of the circuit are much more important than disturbances in the second diffuser even though the latter have less distance to die away before reaching the working section. The concentration of u-component energy in the low frequencies is noticeable in most other tunnels whose turbulence has been measured (with the exception of the R.A.E. 4 ft × 3 ft tunnel where the u-component spectral density at low frequencies is lower, in proportion, than the v and w component densities: probably the 4 ft × 3 ft tunnel's 30 : 1 contraction is responsible for the elimination of practically all the 'unsteadiness', so that the u-component fluctuations in the working section arise from the tendency to isotropy, which naturally makes itself apparent first in the higher frequencies). The contribution at the fan blade frequency (about 80 c/s) seems to be quite small: the height of the peak depends on the filter bandwidth but the energy content is correctly represented, even by a $\frac{1}{3}$-octave plot.

The lateral and vertical components are more than twice as large as the longitudinal component, again following the behaviour observed in other tunnels. Some at least of the peaks in the spectra were caused by eddy shedding from the hot wire probe and its supports: the 50 c/s peaks can be attributed to hum pickup. The fan blade frequency falls in the passband of the 80 c/s filter. Redesign of the hot-wire probes to eliminate the spurious peaks would have occupied more staff and tunnel time than was warranted.

The turbulence intensities are of course very satisfactory, and permit the tunnel to be used for laminar-flow stability investigations as well as turbulence studies. Some measurements of the weak irrotational fluctuations outside a turbulent boundary layer are reported in Ref. 11. The use of a honeycomb and a total of six screens is justified, even for turbulence work, by the resulting insensitivity of the flow in the working section to separations in the diffuser: tunnel operation is therefore easier because careful control of the diffuser blowing is not necessary, and in fact the tunnel has usually been run with no blowing at all.

The roof boundary layer (Fig. 12) is, as mentioned above, thicker than the boundary layer on a smooth surface. The sidewall boundary layers in zero pressure gradient (Fig. 13) show evidence of pronounced secondary flow, which seems to be much stronger than in fully developed duct flow. Although the boundary layer halfway up the sidewall is over 5 in. thick, the $U/U_\infty = 0{\cdot}9$ contour is only about $1{\cdot}7$ in. from the surface at this position (compared with $1{\cdot}3$ in. in the case of the roof boundary layer) and the boundary layer elsewhere on the sidewall is much thinner. It may be assumed that the flow in the corners themselves—which is responsible for any departure from two-dimensionality of the flow in the floor boundary layer—is much the same as in an isolated corner. The surface shear stress on the floor at $x = 65$ in. *not* $x = 93$ in. is shown in Fig. 14: it becomes constant at not more than four boundary-layer thicknesses from the sidewall ($z = 5$–6 in. say). Before the tunnel was built, a rather ill-conducted experiment was done on the flow in the corner between two perpendicular flat plates: the results were similar to those of Fig. 14 and the work reported in Ref. 12. In adverse pressure gradients, the secondary flow becomes weaker because the secondary-flow vortices are compressed longitudinally, leading to the familiar phenomenon of premature separation in corners. It would have been interesting to explore the flow in more detail but the results would not have been directly applicable to smooth-walled ducts.

Flow in the First Diffuser.

Approximate total-pressure profiles just ahead of the first corner, based on a small number of traverses, are shown in Fig. 15a: in this case, the working-section roof was set to give zero pressure gradient with sealed sidewall slots, and no tangential blowing air was supplied, so that the flow through the leading-edge bleed was compensated by inflow through the breather slots. Naturally, there is a large region of separated flow near the roof of the diffuser and the static-pressure recovery coefficient is only about $0{\cdot}35$ (diffuser area ratio $1{\cdot}73$: ideal static-pressure recovery coefficient $0{\cdot}67$). The flow in the working section is still adequately steady but the top speed of the tunnel is considerably reduced, and the large inflow of atmospheric air tends to introduce dust. The application of tangential blowing raises the pressure recovery as shown in Fig 15b. In zero pressure gradient, the tunnel is normally run with a blowing dynamic pressure Δb of $3\Delta p_{\text{ref}}$ in the roof jet and $1{\cdot}1\ \Delta p_{\text{ref}}$ in the floor jet: if the air were supplied by a perfectly efficient compressor the power-factor increment would be $0{\cdot}03$, and the decrease in power factor achieved by blowing is about $0{\cdot}1$. The total-pressure contours for $\Delta b_{\text{roof}}/\Delta p_{\text{ref}} = 3$, $\Delta b_{\text{roof}}/\Delta b_{\text{floor}} = 2{\cdot}73$ are shown in Fig. 15c.

Flow in the Fan Section.

The flow approaching the fan has been explored more thoroughly (Fig. 16): it is much more nearly uniform than that ahead of the first corner. There appear to be regions of low total pressure near the edges of the horizontal faces indicating that the spanwise distribution of tangential blowing is over-concentrated near the centre line (the blowing ducts are fed through single pipes on the centre line as this was found to produce a better flow distribution ahead of the first corner than feeding through three pipes spaced along the span: in fact this is overdoing it). It also appears that the total blowing momentum is somewhat too small to produce axisymmetric flow. The flow at the end of the fan nacelle (Fig. 17) is much more nearly axisymmetric.

The total-pressure drop caused by the corners cannot easily be separated from that caused by the cross-leg of the diffuser (there is a net static pressure rise coefficient of $0{\cdot}04$ across the first two corners and the cross-leg combined), but as thin sheet-metal turning vanes are perhaps the most

reliable component of a wind tunnel it was not thought necessary to make any careful exploration of the flow over them. The slight lateral asymmetry of the flow approaching the fan can be adequately explained by the wake of the fan shaft fairing and the extra surface-friction losses on the longer outside wall.

The asymmetry is much reduced by the fan itself which, as shown by Preston[13], acts in the same way as a freely-rotating windmill. The traverses shown in Fig. 17 were made only an inch or so downstream of the fan nacelle tail, so that the exact depth of the total-pressure deficit on the centre line is not to be relied on. There may also be some slight influence of the wakes of the nine straightener vanes, the top one of which is exactly vertical and therefore coincides with the line of the traverse. A radial traverse was made between two of the straightener vanes to check that this total pressure deficit was caused by boundary-layer growth on the nacelle rather than stalling of the fan blades near the roots: it does seem that the fan, or pre-rotation vanes are partly responsible, but that the rate of boundary-layer growth on the nacelle is large. It was probably a mistake to allow a net expansion in area over the rear of the fan nacelle but the nacelle wake is not so large as that of the R.A.E. 4 ft × 3 ft tunnel[14], where the centre line velocity 0·3 nacelle lengths downstream of the tail was still less than half of the velocity outside the wake. The jet nozzle in the nacelle tail was covered by a fairing during the measurements, but could be used to eliminate the nacelle wake if desired.

The flow near the tunnel walls remains satisfactorily attached, both in the expansion at the rear of the fan duct and in the change of section from octagonal to square.

Flow in the Second Diffuser.

The velocity profiles ahead of the third corner (Fig. 18) indicate that the vertical asymmetry observed fore and aft of the fan has become noticeably worse. The flow in this part of the tunnel is probably rather sensitive to the tangential blowing pressure, which was not automatically controlled during the measurements and may have varied by $\pm 3\%$, at the most, so that the results may not be significant. The lateral asymmetry, on the other hand, has just disappeared: this is more likely to be due to the delayed results of under-turning at the first and second corners than to instability of the flow in the diffuser, since the tests on the R.A.E. 4 ft × 3 ft tunnel[15] suggested that asymmetries in a 5° octagonal diffuser of about the same area ratio were neutrally stable. Actually the velocity in the corners of the square diffuser is no lower than at the mid-points of the sides so it appears that nothing has been lost by this concession to constructional simplicity. Earlier tests with the temporary working section and an inferior distribution of tangential blowing indicated that there were low-velocity regions in the corners although the flow was still well attached: probably, this can be blamed on inadequate blowing. The only other measurements of flow in square diffusers seem to be those in the R.A.E. No. 2 $11\frac{1}{2}$ ft × $8\frac{1}{2}$ ft tunnel: there (Fig. 28 of Ref. 16) the flow in the corners seemed to be no worse than the flow nearer the centres of the walls. It is interesting to note that the velocity near the sidewalls is less than near the top and bottom walls, the opposite of the state of affairs before the fan. Very detailed measurements of the turbulence intensities and shear stress would be needed to explain all these results fully, and the extra work is not warranted.

Flow in the Settling Chamber.

No measurements have been made of the flow in the wide-angle diffuser because this section is not easily accessible. As mentioned above, the turbulence intensity near the floor downstream of all the screens decreased when the honeycomb was moved 6 in. further downstream of the wide-angle diffuser and there is now no suggestion of poor flow in this region.

The turbulence level in the contraction measured with 20 mesh, 28 g. screens is shown in Fig. 19. The increase in turbulence intensity above the Reynolds number $Ud/\beta\nu$ of 80 at which eddy shedding begins can be clearly seen: the decay of turbulence with increasing distance from the screen is also apparent. The u-component spectrum at 22 in. from the last screen and at a tunnel speed of 120 ft/sec shows a high-frequency cutoff proportional to (frequency)$^{-7}$ approximately, as predicted by Heisenberg: there is no trace of the eddy-shedding frequency or of any other discrete frequency apart from the 50 c/s mains frequency and its harmonics picked up by the electronics.

The mean flow at the start of the working section has not been measured because the satisfactory flow in the return circuit leaves little doubt that no large static-pressure variations exist, and because the total-pressure variations can be measured much more accurately in the settling chamber.

A number of measurements have been made in the contraction boundary layer to investigate the rather disappointing failure of the layer to revert to the laminar state in the region of rapid acceleration, but only the velocity profile at the contraction exit (Fig. 20) is of any general interest.

Miscellaneous Tests.

(i) *Temperature rise.*—Small closed-circuit wooden tunnels suffer from a large rise in temperature on prolonged running: this is a disadvantage when hot wires are being used because the wire calibration is a function of temperature. The introduction of cold compressed air into this particular tunnel has a noticeable effect on the temperature rise but with the usual blowing quantities a difference of roughly 40°C between the temperature of the compressed air and that of the atmosphere would be required to cancel it altogether. The temperature rise during measurement runs is minimised by running the tunnel at full speed, without blowing, for a few minutes beforehand: the variation of temperature with time at a speed rather below the maximum is shown in Fig. 21. It can be seen from a semi-logarithmic plot that the temperature rise can be described by at least three time constants, of roughly 30, 60 and 80 minutes. The calculated rate of temperature rise of the air neglecting *all* heat loss is 9°C per minute whereas the actual rate observed immediately after starting is only about 0·6°C/min. so that even the smallest time constant represents the heating of the most highly conducting parts of the tunnel structure (the aluminium floor of the working section for instance) rather than the air itself. The heating up of the heavy screen frames and the other thick timbers is very much slower. The results are rather inaccurate at large times because of the increase in temperature of the tunnel room (only partly due to the heat emitted by the tunnel): the final temperature of the tunnel was about 9°C above atmospheric.

(ii) *Sound level in the settling chamber.*—The mean-square sound pressure level (Fig. 22) is proportional, at the higher speeds, to about the 4·7th power of speed. It appeared, from listening to the noise in the settling chamber, that radiated noise greatly outweighed turbulence in the airstream. Spectrum measurements show that broad-band noise radiated by turbulence (presumably the irreducible turbulence from the working-section boundary layers) contributes more to the sound than do the pulsations at the fan blade frequency and its harmonics, a very satisfactory result. Measurements of surface-pressure fluctuations in the working section show that the low-frequency end of the surface-pressure fluctuation spectrum is swamped by sound, apparently propagating upstream from the diffuser boundary layers. Similar spurious contributions to the spectrum have been found in many other tunnels.

Test Conditions.

Unless otherwise stated, the graphs refer to the following test conditions:

zero pressure gradient, roof and wall suction slots sealed

working-section speed 130 ft/sec (reference pressure difference $\Delta p_{\text{ref}} = 4$ in. of alcohol)

leading-edge height 0·25 in.

suction holes in contraction sealed

tangential-blowing dynamic pressure 10 in. water (roof), $\dfrac{\Delta b_{\text{roof}}}{\Delta b_{\text{floor}}} = 2{\cdot}73$

fan-nacelle tail jet faired.

All the mean flow measurements were made with 20 mesh 28 s.w.g. screens fitted, unless otherwise stated. The turbulence measurements in the working section were made with 16 mesh 28 s.w.g. screens fitted (the present arrangement).

Conclusions.

The performance of the tunnel is extremely satisfactory, both aerodynamically and mechanically. The mean flow and turbulence level are very good indeed and the efficiency of the smoothing arrangements enables great liberties to be taken in the working section without the tunnel flow becoming unsteady. The honeycomb, in particular, has well merited its inclusion. The use of the flexible roof has proved very easy, except for the tedium of cutting the side sealing strips to length. The only improvements that one could wish for would be the redesign of the slot entry shapes to reduce the boundary-layer growth on the roof and sidewalls, and the replacement of the contraction by one of more conventional shape, also to reduce boundary-layer growth and so reduce the required bleed under the leading edge. The first stages of the study of turbulent boundary layers now in progress are reported in Refs. 11, 17 and 18.

Acknowledgements.

Most of the wooden and fibreglass structure of the tunnel was made by J. B. Freed and R. Woods, under the direction of E. A. Frankland, and they were also responsible for much of the assembly work, including the working section roof. We particularly wish to acknowledge their skill and patience in dealing with difficulties not of their making. The fan was made by R. Coad and P. Oinn. The metal parts of the structure were made under the direction of L. Lambert.

NOTATION

F	Mean-square spectral density per c/s: $\int_0^\infty F\,df = 0{\cdot}231.\,Ff$ plotted.
f	Frequency, c/s
H	Boundary-layer shape factor δ_1/δ_2
p	Static pressure
U	Velocity in x direction
x, y, z	Co-ordinates: origin at leading edge on centre line x streamwise, y vertical
z^1	z measured from sidewall
β	Ratio of open area of screen to total area
Δp_{ref}	Pressure difference between ends of contraction
Δb	Dynamic pressure of tangential-blowing jet
δ_1	Boundary-layer displacement thickness
δ_2	Boundary-layer momentum thickness

Suffixes

0	Conditions at 15°C, 760 mm. Hg.
1	Edge of boundary layer
ref	Based on pressure difference between ends of contraction.

REFERENCES

No.	*Author(s)*	*Title, etc.*
1	F. H. Clauser	Turbulent boundary layers in adverse pressure gradients. *J. Ae. Sci.*, Vol. 21, p. 91. 1954.
2	P. Bradshaw and R. C. Pankhurst	The design of low-speed wind tunnels. N.P.L. Aero. Report 1039, 1963 and *Prog. Aero. Sci.*, Vol. 5, p. 1. 1964.
3	V. A. Sandborn..	Preliminary experimental investigation of low-speed turbulent boundary layers in adverse gradients. N.A.C.A. Tech. Note 3031. October, 1953.
4	Staff of Aero. Division, N.P.L...	On the measurement of local surface friction on a flat plate by means of Preston tubes. A.R.C. R. & M. 3185. May, 1958.

REFERENCES—*continued*

No.	*Author(s)*	*Title, etc.*
5	W. A. Mair	The design of fans and guide vanes for high-speed wind tunnels. A.R.C. R. & M. 2435. June, 1944.
6	R. F. Johnson	A simple control system for reversing DC motors using silicon controlled rectifiers. N.P.L. Aero. Report. 1073. 1963.
7	P. Bradshaw	The effect of wind tunnel screens on 'two-dimensional' boundary layers. N.P.L. Aero. Report 1085. A.R.C. 25 402. December, 1963.
8	M. J. Lighthill	A new method of two-dimensional aerodynamic design. A.R.C. R. & M. 2112. April, 1945.
9	J. H. Preston	The minimum Reynolds number for a turbulent boundary layer and the selection of a transition device. *J. Fluid Mech.*, Vol. 3, p. 373. 1958.
10	D. H. Ferriss	Measurements of the free stream turbulence in the R.A.E. Bedford 13 ft × 9 ft wind tunnel. A.R.C. C.P. 719. July, 1963.
11	P. Bradshaw	Irrotational fluctuations near a turbulent boundary layer. N.P.L. Aero. Report 1121. 1964.
12	F. B. Gessner and J. B. Jones ..	A preliminary study of turbulence characteristics of flow along a corner. *Trans. A.S.M.E.*, Vol. 83D, p. 657. 1961.
13	J. H. Preston	The effect of a wind tunnel fan on irregularities in the velocity distribution. A.R.C. R. & M. 2307. September, 1944.
14	H. B. Squire and K. G. Winter..	The R.A.E. 4 ft × 3 ft experimental low turbulence wind tunnel. A.R.C. R. & M. 2690, 2905, 3261.
15	J. A. Lawford	Measurements of velocity fluctuations in the working section of the R.A.E. 4 ft × 3 ft wind tunnel with flow disturbances in the second diffuser. A.R.C. C.P.455. October, 1958.
16	D. C. MacPhail, J. G. Ross and E. C. Brown.	The No. 2 11½ ft × 8½ ft wind tunnel at the Royal Aircraft Establishment. A.R.C. R. & M. 2424. August, 1945.
17	J. A. B. Wills	On pressure fluctuations under turbulent boundary layers. N.P.L. Aero. Report 1131. A.R.C. 26 514. December, 1964.
18	P. Bradshaw and D. H. Ferriss	The response of a retarded equilibrium turbulent boundary layer to the sudden removal of pressure gradient. N.P.L. Aero. Report 1145. A.R.C. 26 758. March, 1965

APPENDIX

Construction

Working Section.

(i) *Frame.*

This frame is made in steel and consists of two end frames (Fig. 3 Part Number 1 ['Fig. 3.1']) connected by two pairs of welded channel sections (Figs. 3.2, 3.4). The lower pair carry the lighter cross-members on which the floor plates (Fig. 3.3) are mounted. The upper pair of channel sections (Fig. 3.4) are bolted in place to support the Perspex wall slats (Fig. 3.5)—which are not directly fastened to the floor—and the jacking arrangements (Fig. 3.6) for the slats (Figs. 3.7, 4.1) which form the flexible roof.

(ii) *Roof.*

The flexible roof is constructed from 58 laminated mahogany slats with aluminium alloy cast end-blocks (Fig. 4.2) attached by sheet metal straps. The outer ends of the end-blocks are faced by P.T.F.E.-coated sheet steel plates (Figs. 3.8, 4.3). On the upper surface of each slat is mounted a slide valve (Fig. 4.4), consisting of an inner and outer brass tube each drilled with 11/32 in. diameter holes at 1 in. pitch over their full length. Each slat is mounted on two spring steel strips (Fig. 4.5) which pass between pairs of cam bearings (Fig. 4.6). The upstream ends of the spring strips are secured to the throat blocks of the settling chamber. In order to allow for changes in the length of strip required in the working section, due to flexing of the roof, the downstream ends of the strips are left free to slide in and out. Flexible seals (Fig. 4.7) made from P.V.C. impregnated nylon cover the gaps between the slats. The downstream edge of each seal is trapped between the upper surface of a roof slat and a brass clamping strip. The upstream edges are similarly held but by the addition of spacing pillars (Fig. 4.8) an air passage is provided (*via* the air valves) to the outside of the tunnel. The flexible seals carry closed-cell rubber sealing strips at their ends and are prevented from buckling by spanwise short-length reinforcing tubes at the ends.

Spindles project from the ends of the roof slats through the $\frac{1}{8}$ in. gaps between the Perspex wall slats, thus constraining the slats to move vertically. The flexible roof is held in position by pairs of external jacks attached to alternate roof slat spindles (Fig. 4.10). The pairs of jack-rods (Fig. 4.10) are threaded at their upper ends into self-aligning jack-nuts (Fig. 4.11). These jack-nuts are mounted on the upper channel sections (Fig. 3.4), and have light chain sprockets attached to their upper faces. The sprockets are connected in pairs by light spanwise chains (Fig. 4.12) supported by a plywood platform. (These light chains are driven by the heavier chain drive described below.) Beneath the plywood platform, and extending the full length of the working section is mounted a steel box section, supported by the transverse members of the upper frame. Spindles mounted in this box section carry chain sprockets at their lower ends and these are linked one to another by a longitudinal loop of chain (Fig. 3.9) supported by nylon strips. This chain loop is driven by a single, $\frac{1}{2}$ h.p., d.c. electric motor, mounted at the upstream end of the box section. To the upper end of each spindle is pinned the lower of a pair of hubs which form part of an electro-magnetic clutch (Fig. 3.10). The upper hub of each clutch is free to rotate with respect to the spindle and has a light chain sprocket attached to its upper face. These sprockets, 28 in all, mesh with the light-weight chain loops which connect the pairs of roof-slat jacks. The clutch energising coil assemblies, which

encircle the pairs of clutch hubs, are mounted on the upper surface of the spindle box. The electromagnetic clutches are energised by a 24 V.d.c. supply controlled by a single switch. The clutches are wired in parallel with two microswitches wired in series between the positive and negative lines which serve the clutches. The upper microswitches limit the downward travel of the pairs of jack-rods.

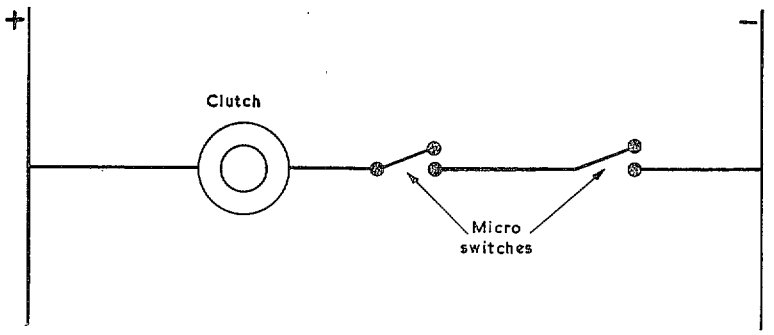

The point at which these microswitches cut off the energising d.c. supply to the clutches is determined by the striker ferrules (Fig. 4.13) which are screwed on to the upper ends of one of each pair of jack-rods. (For safety reasons the striker ferrules are positioned so that the roof slats do not approach closer than 5 in. from the upper surface of the floor, smaller movements being allowed at each end of the roof.) The upper microswitches (Fig. 4.14) are mounted on the edge of the working section's hinged plywood top cover. This cover is hinged to permit resetting of the upper microswitches (when these have been operated) by removal of wedge blocks which support the hinged roof. The lower microswitches (Fig. 4.15) limit the upward travel of the pairs of jack-rods, and are attached to spring-loaded clamps which may be adjusted to any desired height in the $\frac{1}{8}$ in. gaps between the sidewall slats. These spring-loaded clamps are used to preset the desired roof shape. The wall slats bear engraved lines in 1 in. increments over the 9 in. range of the roof travel. The lower microswitch outer clamping plates have attached to one of their edges a scale (Fig. 4.16) 1 in. in height and engraved with 1/10 in. graduations. It is thus possible to record and repeat roof shapes. The lower, moving microswitches are connected to the clutches by self-coiling miniature cables as used in telephone receivers.

(iii) *Floor.*

The floor of the working section is constructed from 6 aluminium alloy cast plates (Fig. 3.3) deeply ribbed on their under sides and having five holes machined in them. Flanged discs ($3\frac{1}{2}$ in. in diameter) (Fig. 3.11) carrying the measuring instruments fit into the holes in the floor plates. Each floor section is mounted on self-aligning bearings, attached to the working section frame, and may be moved in a direction transverse to the airflow by fitting the two floor extension plates and traverse jack (Fig. 3.12). Both of the extension plates have 3 holes, similar to those in the main floor sections; providing additional mounting positions for flanged discs. The use of floor extension plates was chosen in preference to making each plate 6 ft 6 in. long in order to save space and because castings more than 5 ft long would not fit in the available annealing furnace. The upstream end of the floor terminates at a leading-edge section (Fig. 5b.1) mounted on the working section frame *via* robust buffer-brackets. The downstream edge of the section opposes the force applied by the wedge-plate assembly which is mounted at the downstream end of the six floor plates, and is used to clamp

the plates firmly together. The wedge-plate assembly consists of a fixed and a sliding wedge-shaped plate both cast in aluminium alloy. The sliding plate is operated by a screw thread and crank handle from the outside of the working section.

The entry face of the first diffuser carries two blowing boxes; one on the upper diffuser entry frame member (Fig. 5a.2) and one on the lower frame member. These boxes are cast in brass and fitted with steel cover plates. The blowing gap can be adjusted by fitting distance pieces (Fig. 5a.3) of suitable thickness. Air is supplied to the blowing boxes through three pipe connectors of 2 in. diameter spaced across the span of the blowing boxes; normally only the centre pipe on each box is used.

The rest of the construction follows conventional practice and only a brief description need be given.

(iv) *Fan Assembly.*

A welded steel angle frame, bolted to the floor, is used to support the outer ends of three of the cast aluminium pre-rotation vanes, whose inner ends are bolted to a large flange on the fan bearing: this flange also serves to support the nose fairing which is a fibreglass moulding, changing to an aluminium drum at the position of the pre-rotation vanes. The other pre-rotation vanes are also bolted to the flange at their inner ends but at their outer ends are merely araldited into the front section of the fan duct, which is also a fibreglass moulding, made in three sections. The fan was made from laminations of 1 in. thick Honduras mahogany. The rear fairing is of fibreglass, supported from the outer duct by the wooden straightener vanes: three of the vanes carry pipes supplying air to the tail jet. Three bracing wires are fitted at the tail. Photographs of the fan and of the stator vane assemblies are published in Ref. 2.

(v) *Settling Chamber.*

There is a cloth seal, acting as an anti-vibration joint, upstream of the rapid expansion. The rapid expansion contains two screens, in frames which can be slid in and out. The frames containing the honeycomb and the main screens are each of 6 in. length, 4 in. thick: they form the tunnel load-bearing structure as well. They are fitted with castors, and raised into position by jacks. Tubular rubber seals are fitted. The whole assembly is clamped together by drawbolts between the rapid expansion and the contraction. Clearance for removal of a frame is obtained by pushing the rapid-expansion section back against the anti-vibration joint.

(vi) *Contraction.*

This is supported by a welded steel frame. The vertical (plane) walls are plywood, and the curved surfaces are of wooden sandwich construction. A former was made for each section, a sheet of ply bent over it, adjacent square strips of wood glued along the generators, and a second sheet of ply laid on top to complete the sandwich. Spring-back was found to be negligible. The final convex curvature at the downstream end is made up by two mahogany throat blocks.

(vii) *Corner Vanes.*

These are 16 g. 99% pure aluminium pressings: the press tool is shown in Fig. 6. The vane spacing and alignment is maintained by C-shaped packing pieces glued in troughs in the floor and roof of the vane frames: the vanes are braced at their leading edges to eliminate all vibration.

(viii) *Diffusers.*

The general method of construction is adequately indicated by Figs. 8 and 9. Tubular rubber seals are provided between sections and round the hatchways. The wooden sections of the tunnel are all finished internally with Phenoglaze phenolic lacquer. The exterior, and the metal frames, are oil painted. It may be of interest to remark that some of the timber used came from the old Duplex tunnel (built 1919).

Fuller details of the return-circuit construction are available from the N.P.L. as a service for designers of other tunnels.

TABLE 1

Contraction Ordinates

	(wide end)									
x (in.)	−56·85	−32·42	−18·71	−8·56	−1·13	+5·40	+10·48	+15·34	+19·18	+23·10
$\pm y$ (in.)	54	53·85	53·70	53·55	53·40	53·24	53·09	52·94	52·78	52·62
x	37·40	47·68	55·92	62·77	68·78	74·04	78·82	83·04	86·87	90·18
$\pm y$	51·80	50·89	49·87	48·71	47·39	45·89	44·19	42·29	40·18	37·91
x	93·12	95·54	97·60	99·17	100·43	101·30	101·93	102·34	102·59	102·76
$\pm y$	35·50	32·98	30·44	27·92	25·50	23·20	21·08	19·15	17·43	15·89
x	102·86	102·94	103·02	103·12	103·25	103·45	103·69	104·03	104·46	105·02
$\pm y$	14·48	13·10	12·1	11·08	10·34	9·43	8·84	8·04	7·52	6·79
x	105·79	212·70	107·21	107·54	107·92	108·35	108·88	109·51	110·32	111·50
$\pm y$	6·32	5·62	5·51	5·40	5·28	5·18	5·06	4·95	4·83	4·72
		(narrow end)								
x	113·50	120·00								
$\pm y$	4·61	4·50								

The contraction is truncated at $x = 0$: the floor and roof are parallel upstream of this. The last screen is at $x = -6$.

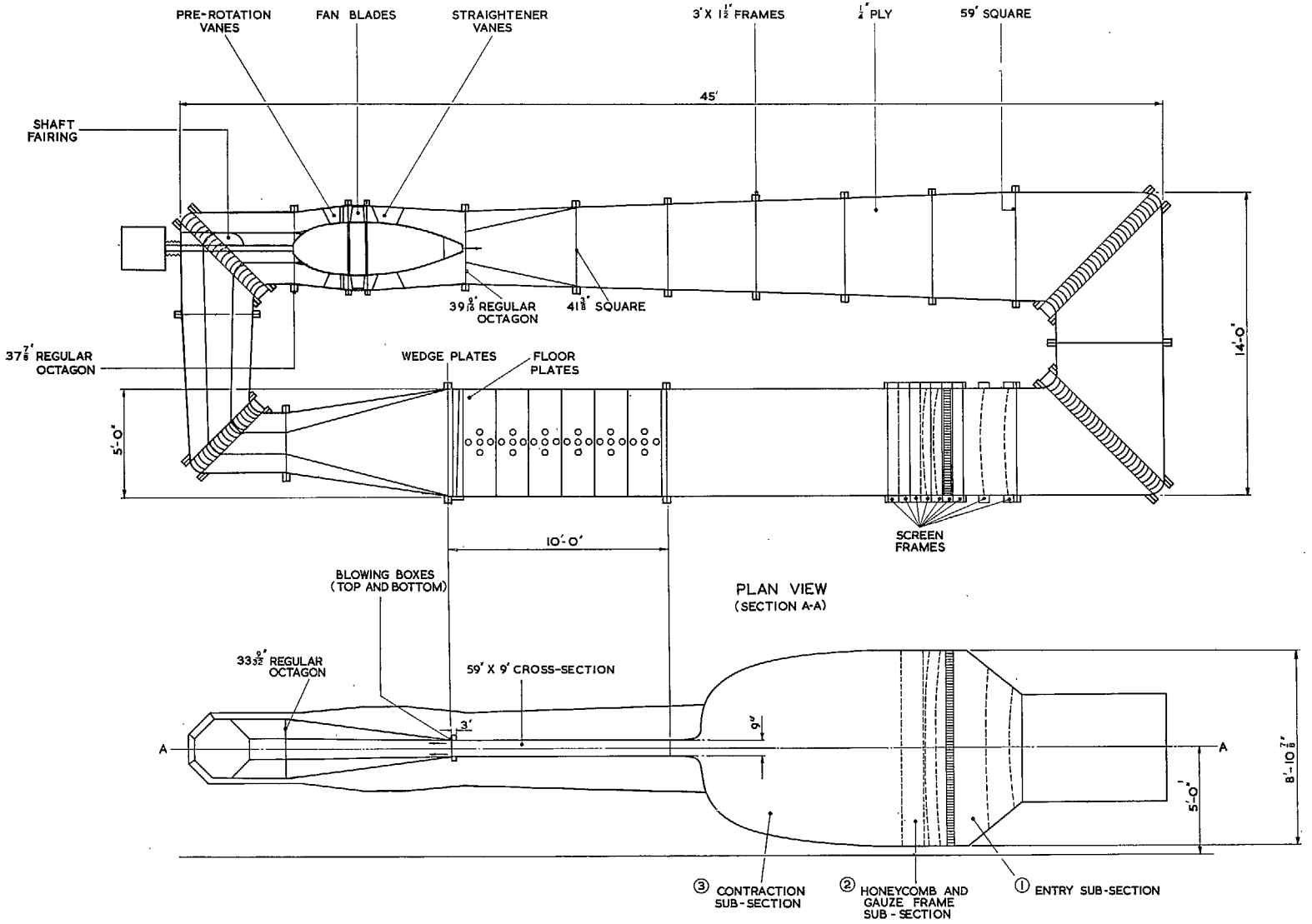

FIG. 1. Side view. (Airline dimensions).

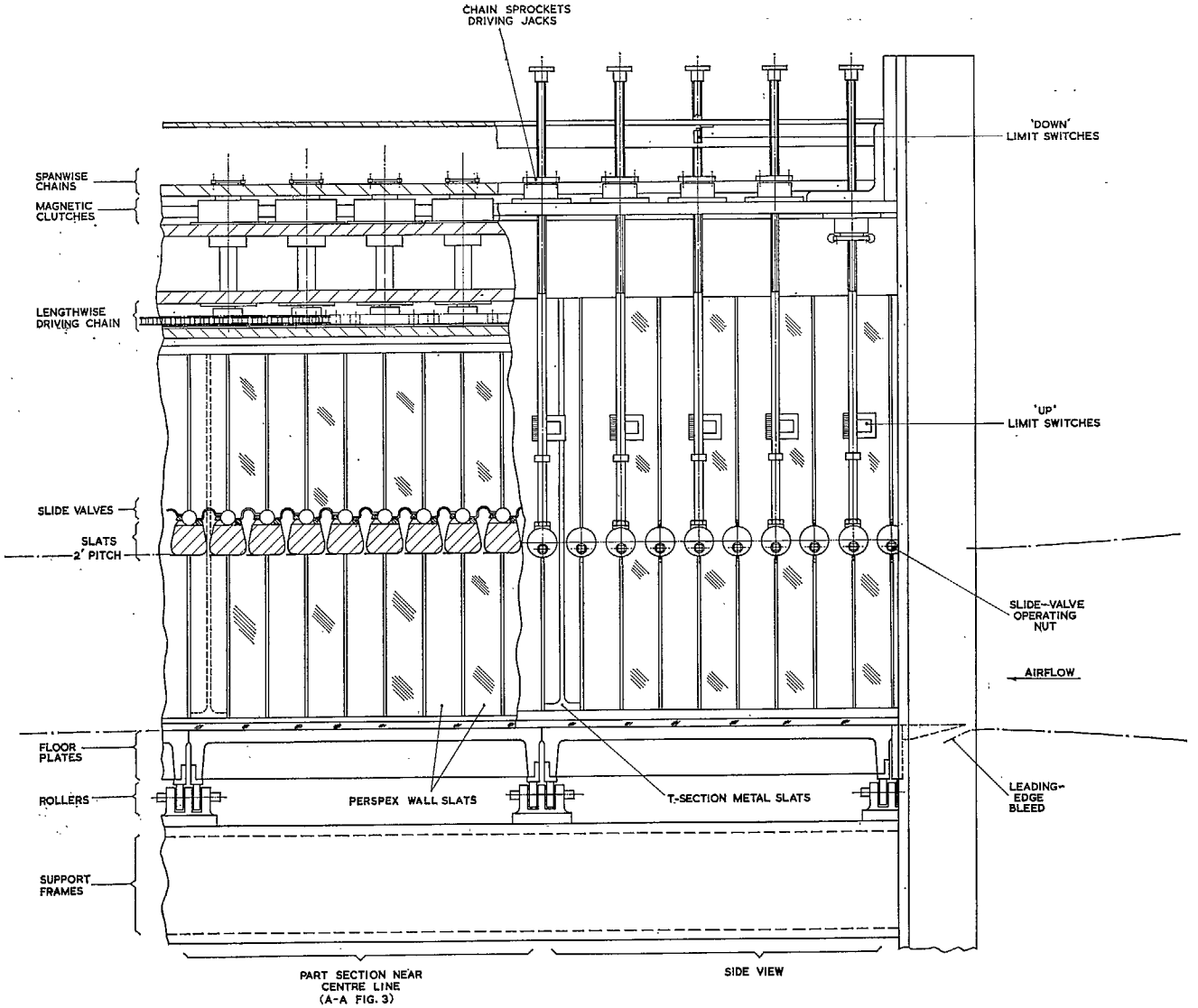

FIG. 2. Working section.

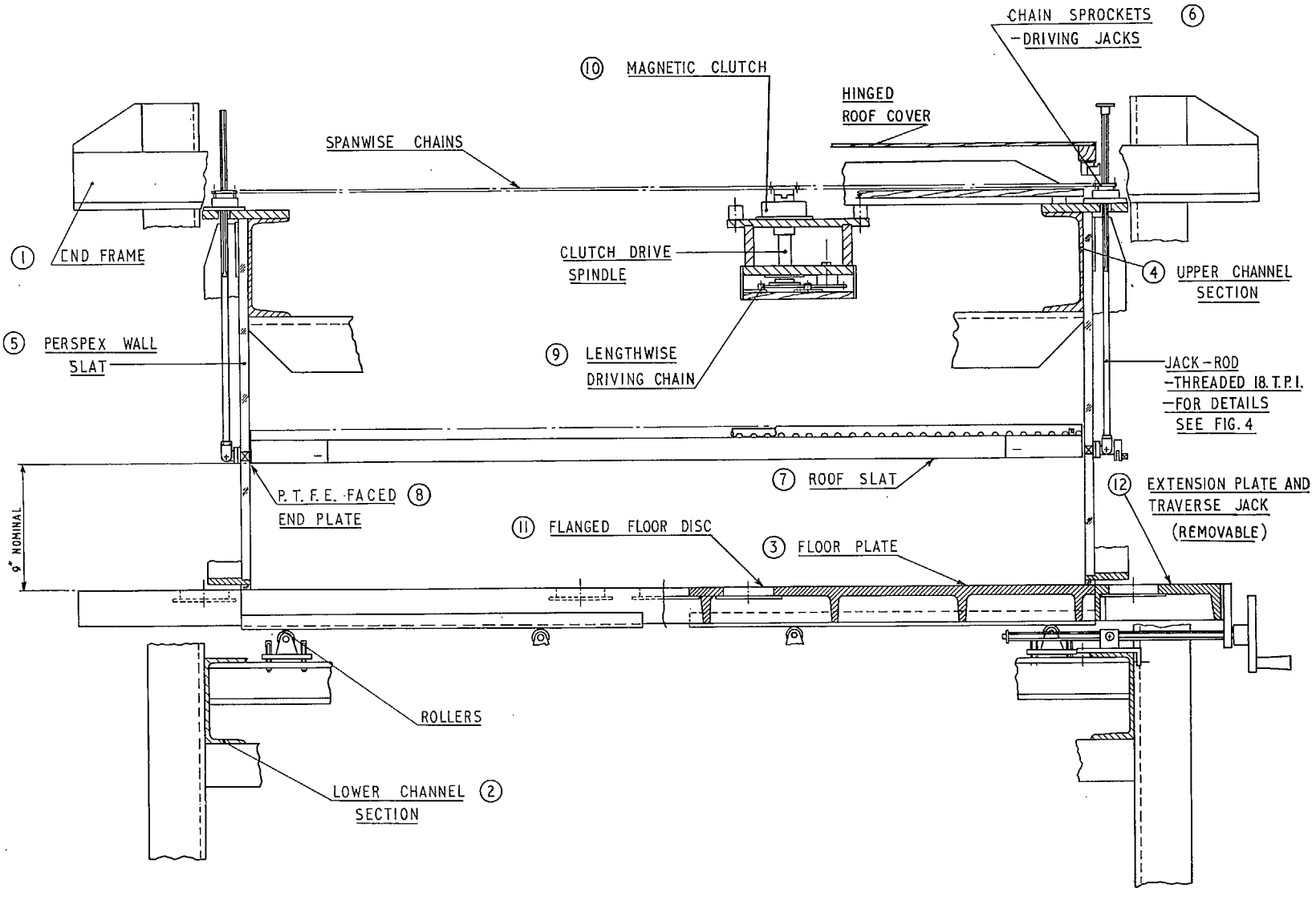

FIG. 3. Cross-section of working section at a slat position.

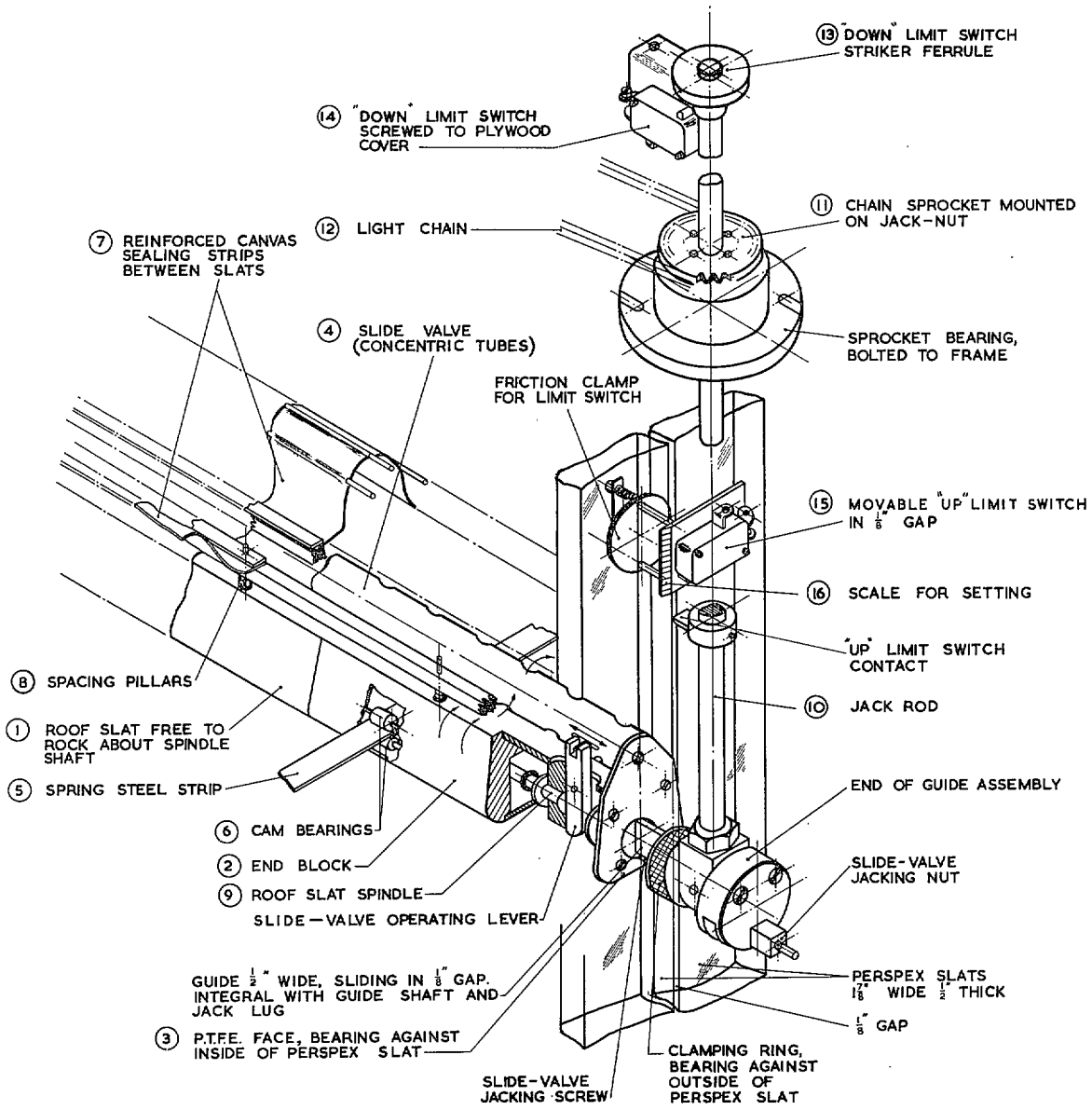

FIG. 4. W.S. roof slat and jack assembly.

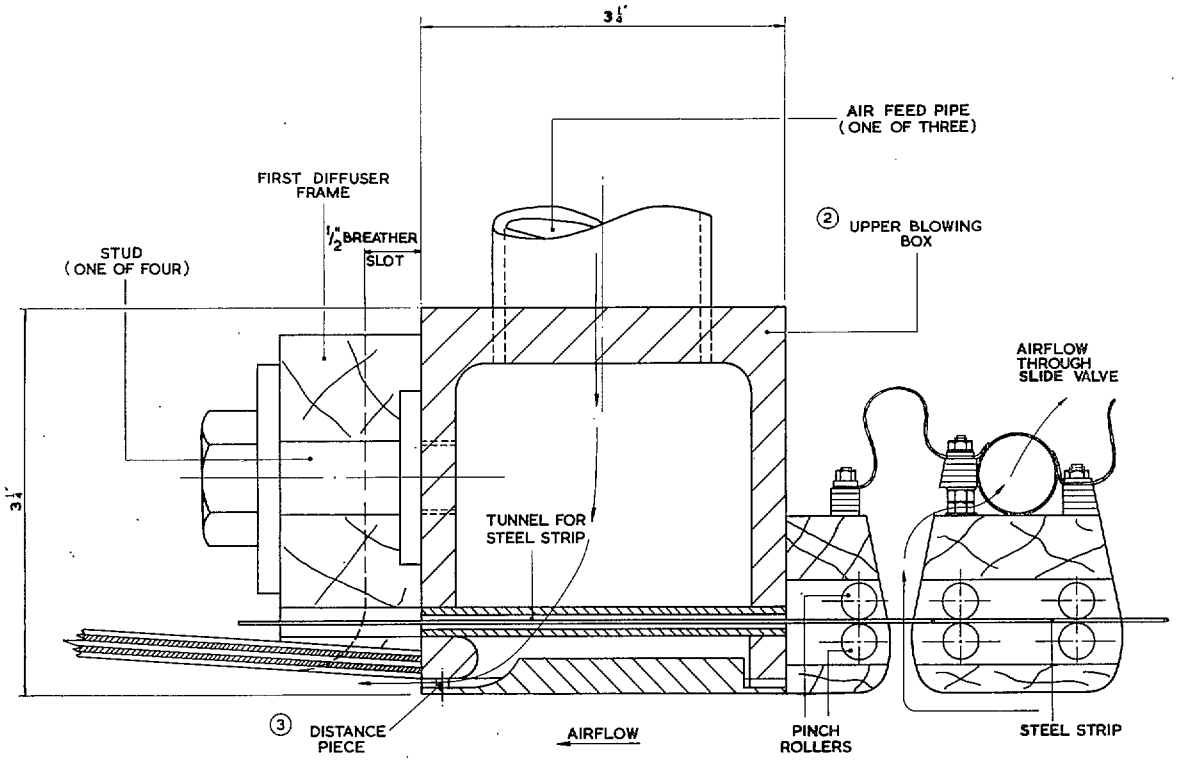

FIG. 5a. Upper blowing box.

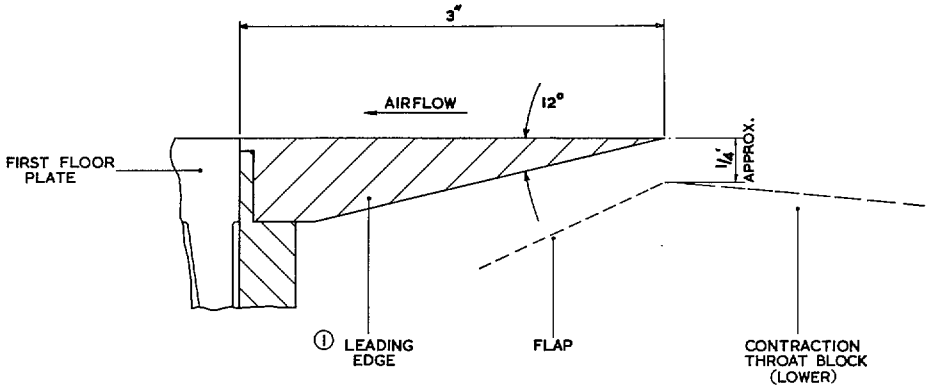

FIG. 5b. Leading-edge section.

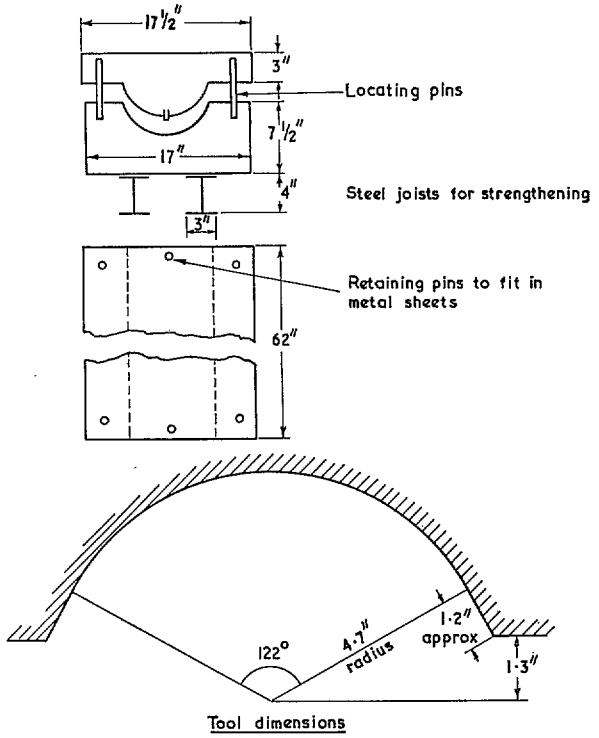

Vane dimensions: Arc length 12" (10" circular arc with 1" straight extensions at leading and trailing edges) Radius 6·67", Chord 10·64"
Material _____ 99% aluminium, 16 s.w.g.
Press load _____ 1 ton
The tool dimensions to allow for springing back were found by a trial with a sample of the material used, but should be fairly accurate for other samples of pure aluminium

FIG. 6. Press tool for 12 in. arc length 86° corner vanes. Material—laminated mahogany.

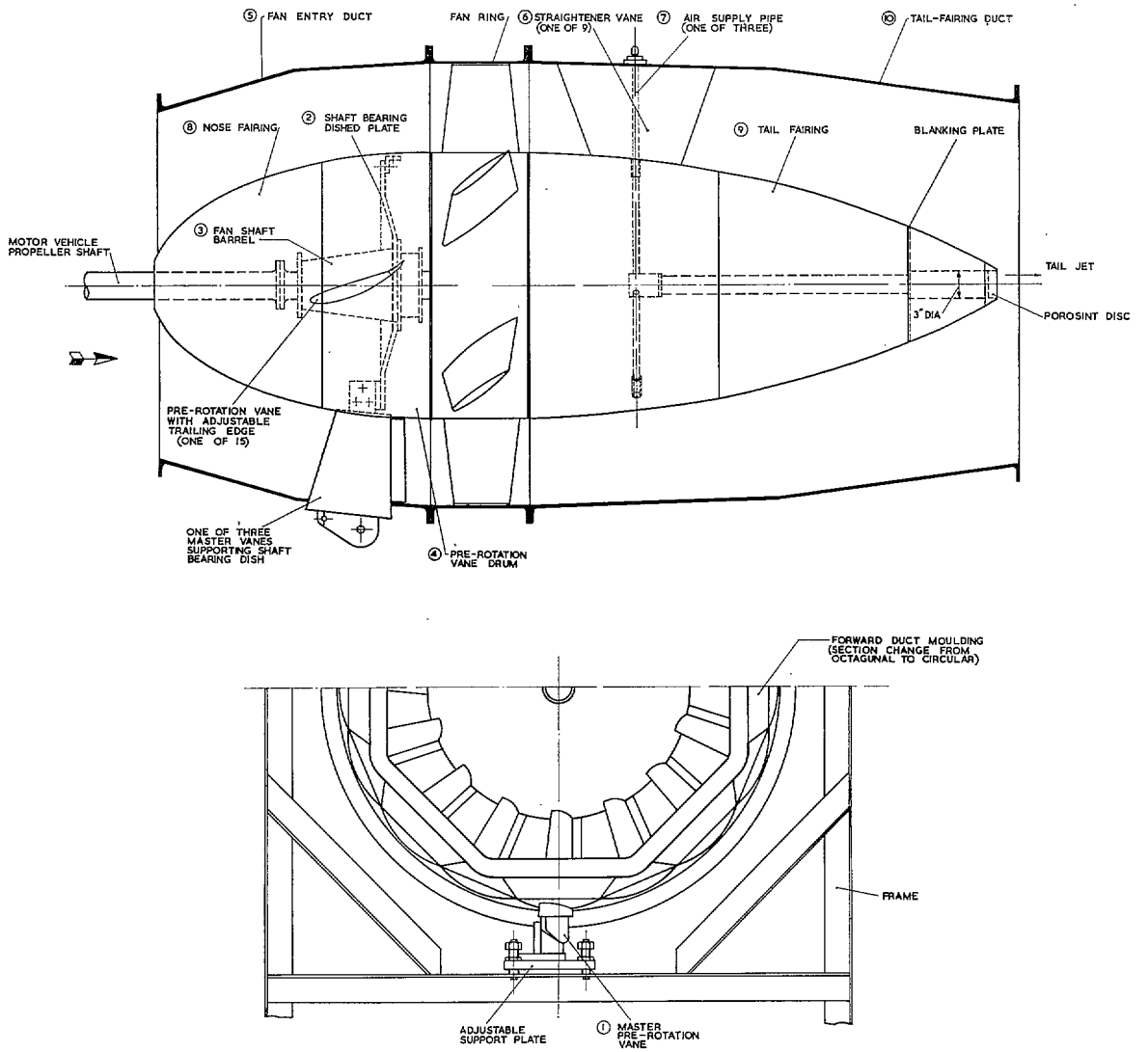

FIG. 7. Fan assembly.

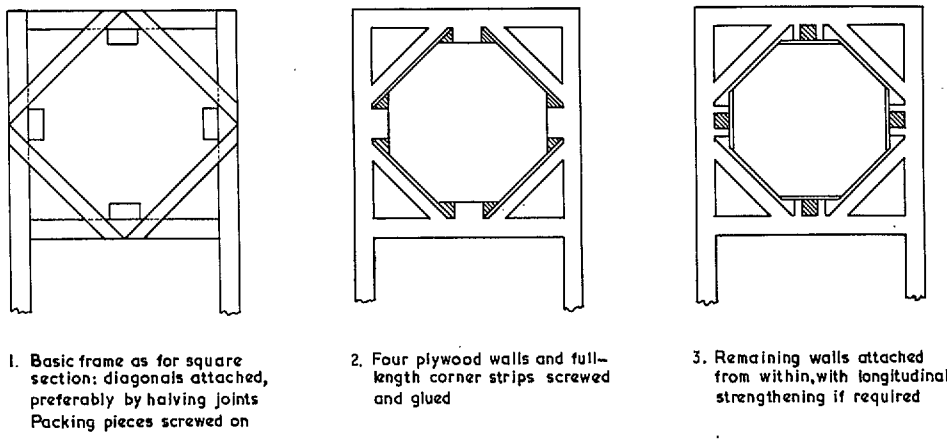

FIG. 8. Stages in construction of octagonal sections.

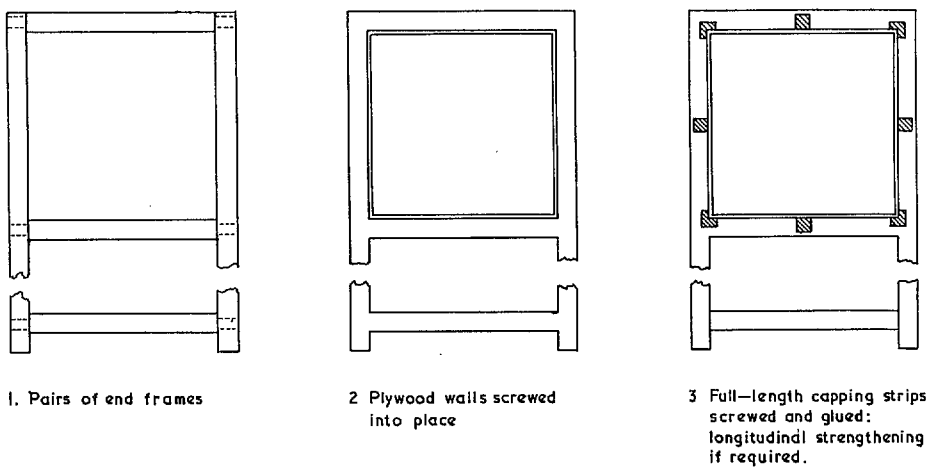

FIG. 9. Stages in construction of square sections.

Main frames 3 in. × 1½ in., plywood ¼ in., longerons 3 in. × 2 in. (max. cross-section 5 ft square, section length 5 ft, internal pressure 30 lb/sq. ft).

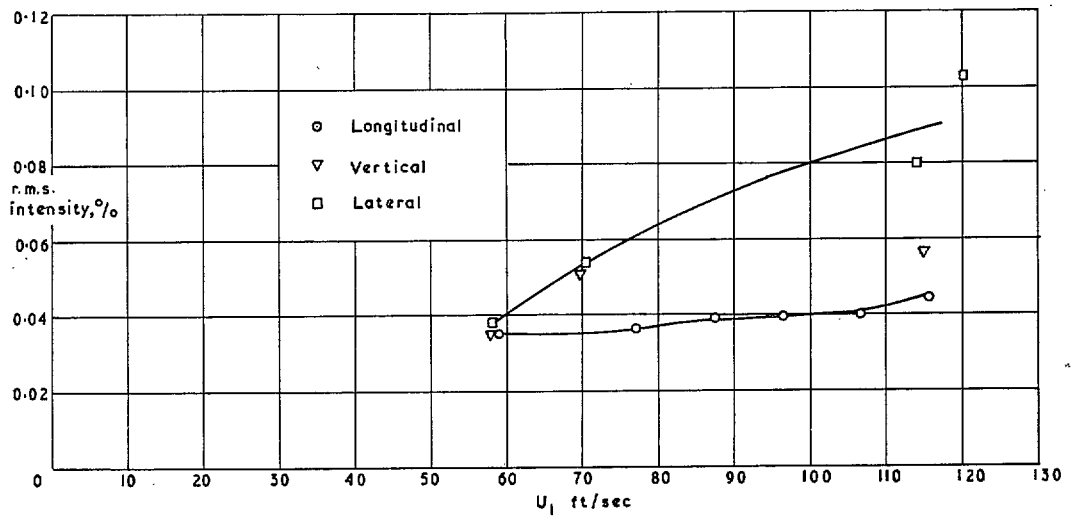

FIG. 10. R.M.S. turbulence intensity in working section. $x = 12$ in.

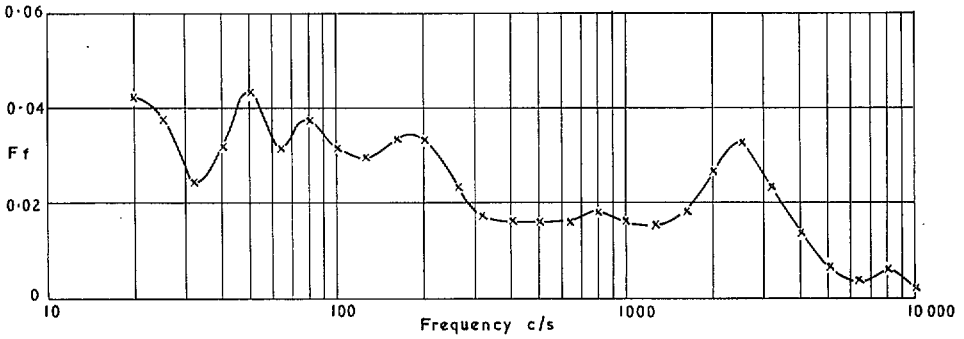

FIG. 11a. Spectrum of longitudinal component of turbulence in working section: $x = 12$ in.; $U_1 = 120$ ft/sec.

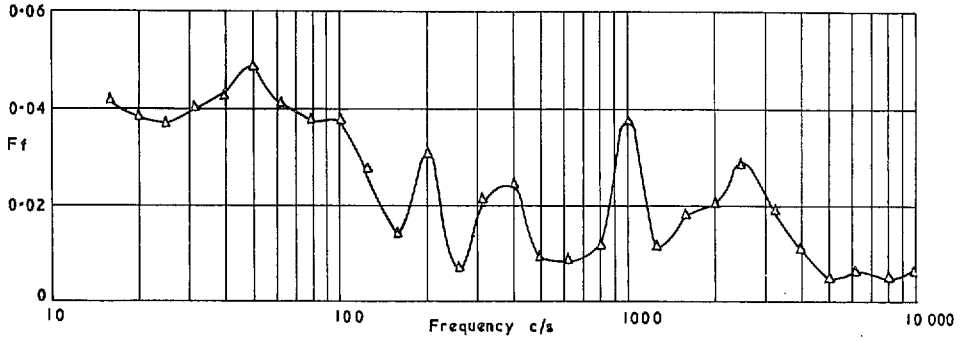

FIG. 11b. Spectrum of vertical component of turbulence in working section: $x = 12$ in.; $U_1 = 120$ ft/sec.

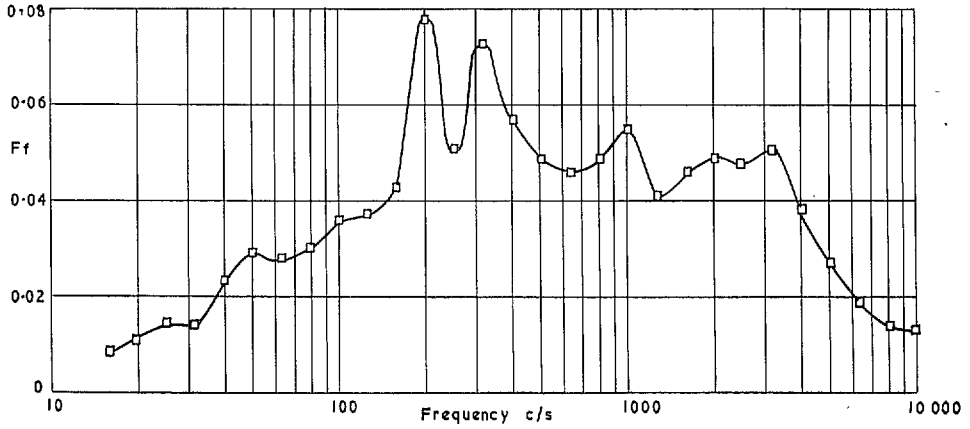

FIG. 11c. Spectrum of lateral component of turbulence in working section: $x = 12$ in.; $U_1 = 120$ ft/sec.

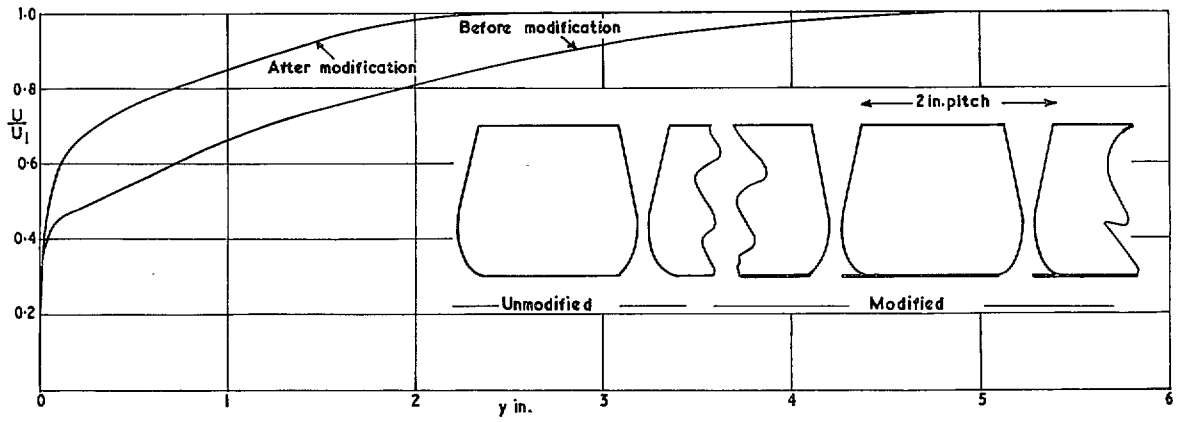

FIG. 12. Boundary-layer profiles on roof of working section before and after modification of slots: $x = 93$ in., $U_1 x/\nu = 6{\cdot}1 \times 10^6$.

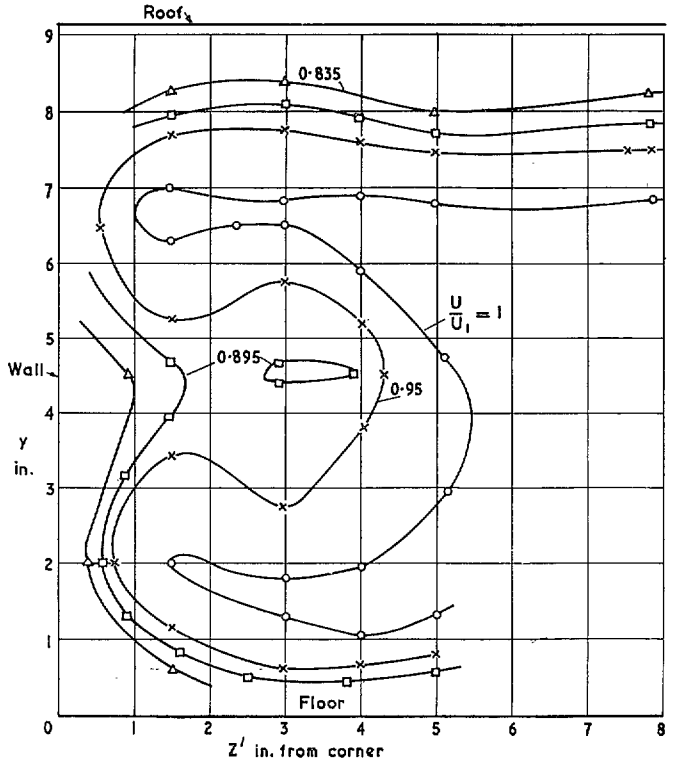

FIG. 13. Velocity contours in corner of working section: $x = 93$ in., $U_1 x/\nu \doteq 6{\cdot}4 \times 10^6$.

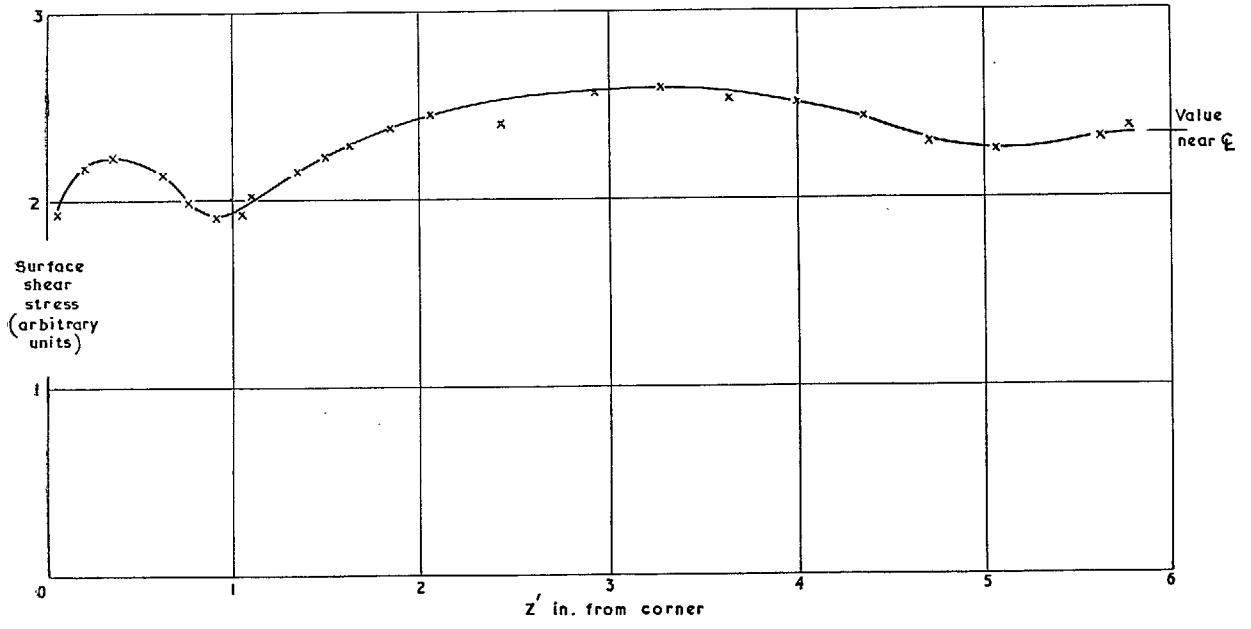

FIG. 14. Surface shear stress in corner of working section: $x = 65$ in.

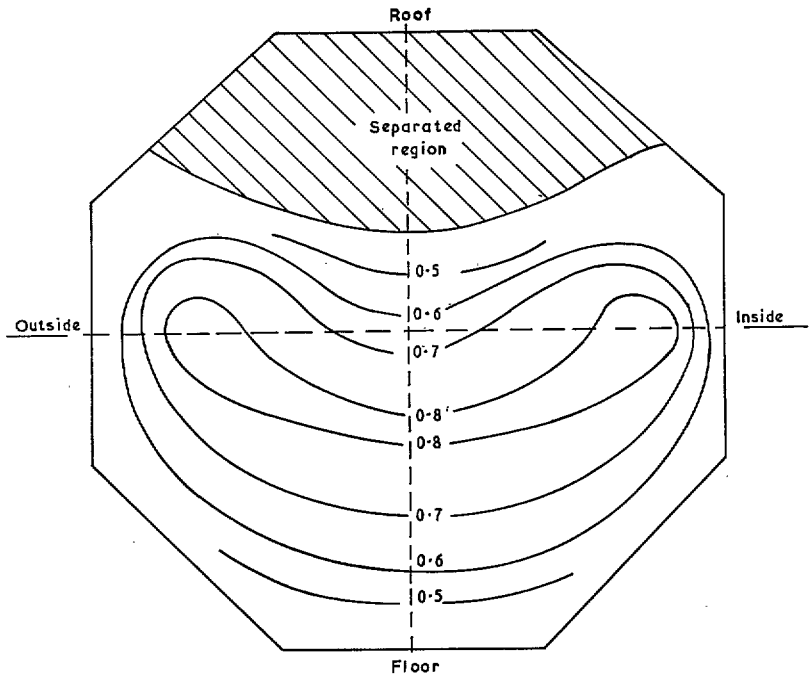

FIG. 15a. Velocity contours upstream of first corner *without* tangential blowing. (Figures are values of U/U_{ref}: traverse lines are shown dotted.)

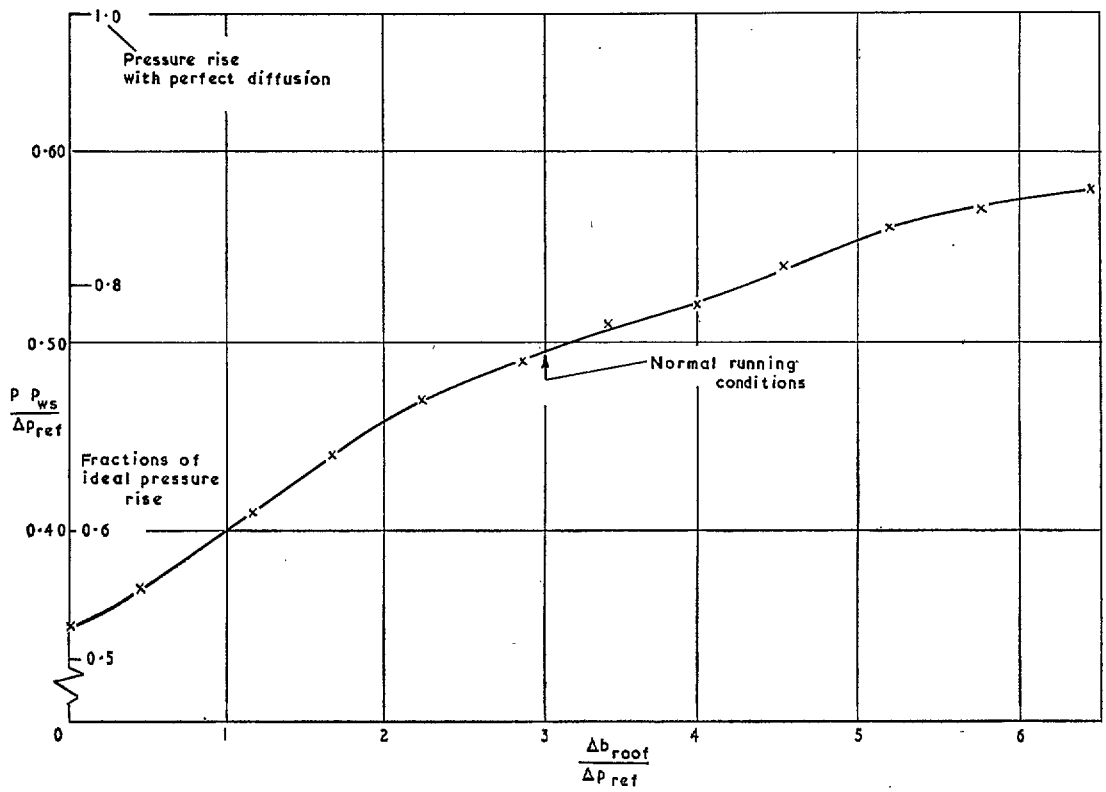

FIG. 15b. Variation with longitudinal blowing pressure of static pressure rise in first diffuser (Area ratio 1·73).

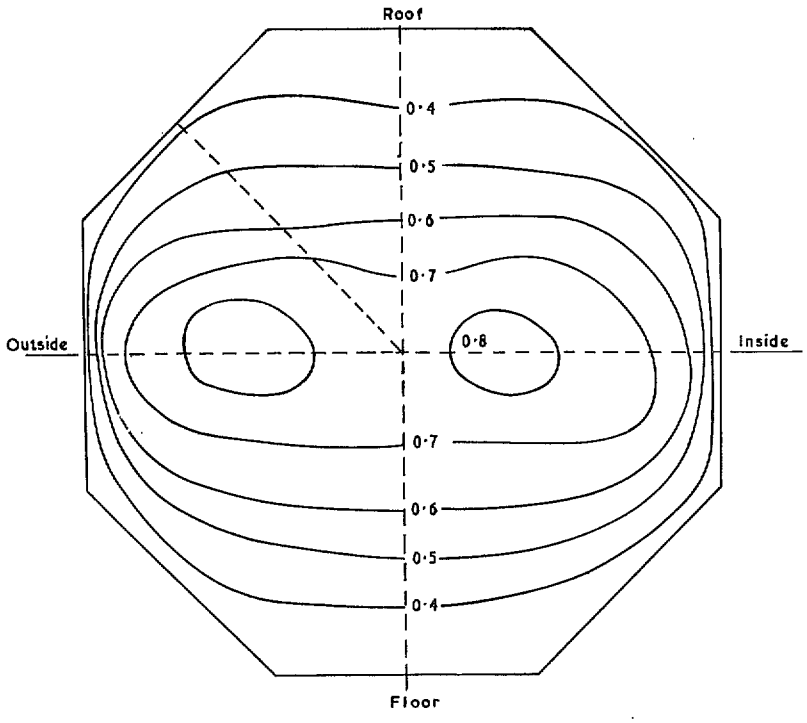

FIG. 15c. Velocity contours upstream of first corner with optimum tangential blowing. (Figures are values of U/U_{ref}: traverse lines shown dotted).

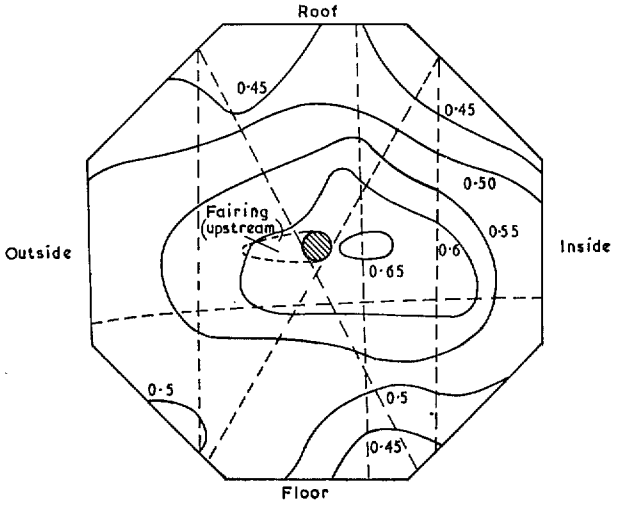

FIG. 16. Velocity contours upstream of fan nacelle. (Figures are values of U/U_{ref}: traverse lines shown dotted).

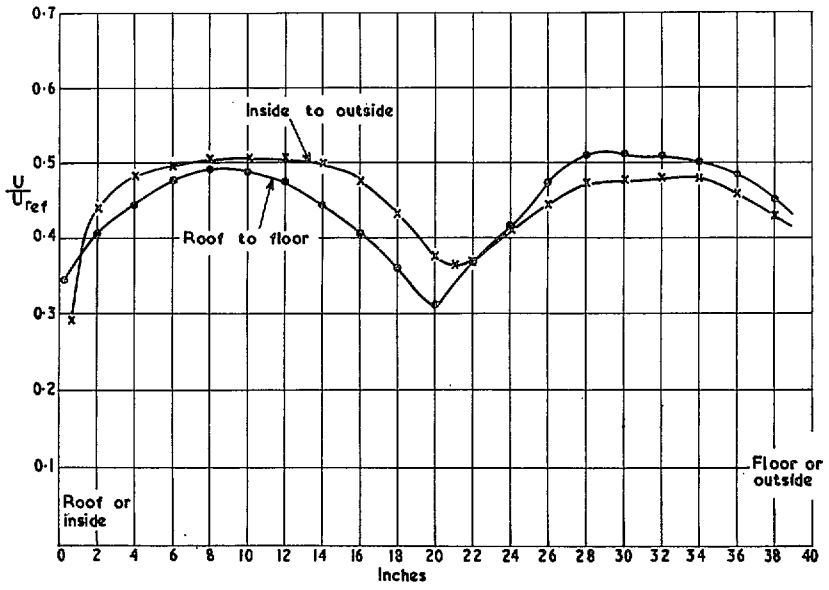

FIG. 17. Velocity profiles just downstream of fan nacelle.

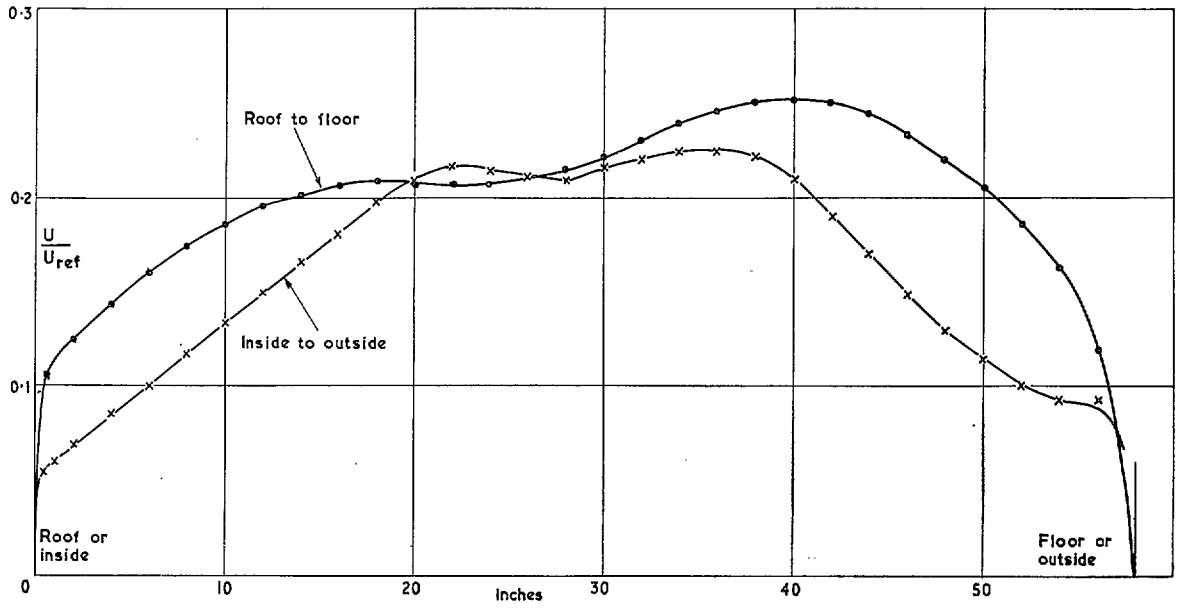

FIG. 18. Velocity traverses just upstream of third corner.

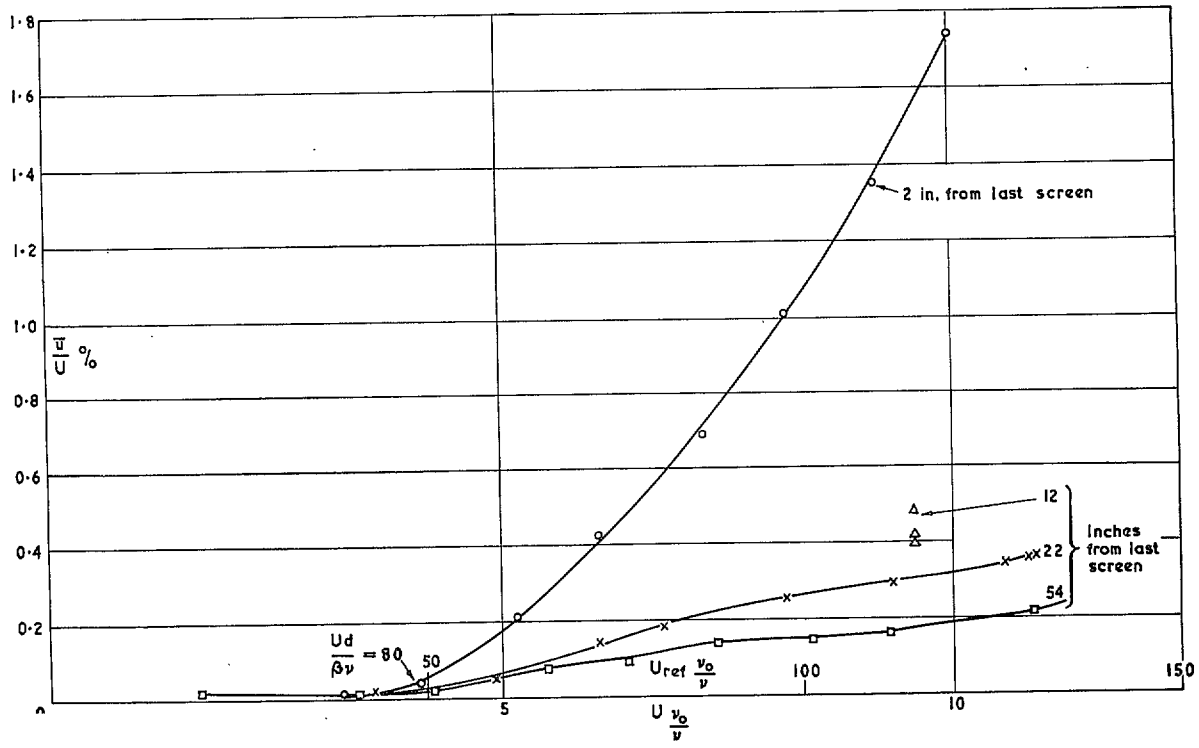

FIG. 19. Turbulence in settling chamber 20 mesh, 28 s.w.g. screens.

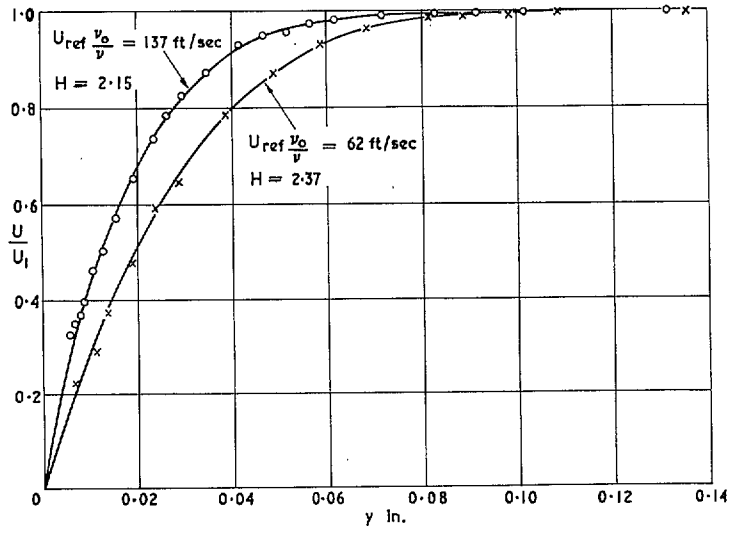

FIG. 20. Boundary layer on contraction floor just upstream of leading edge.

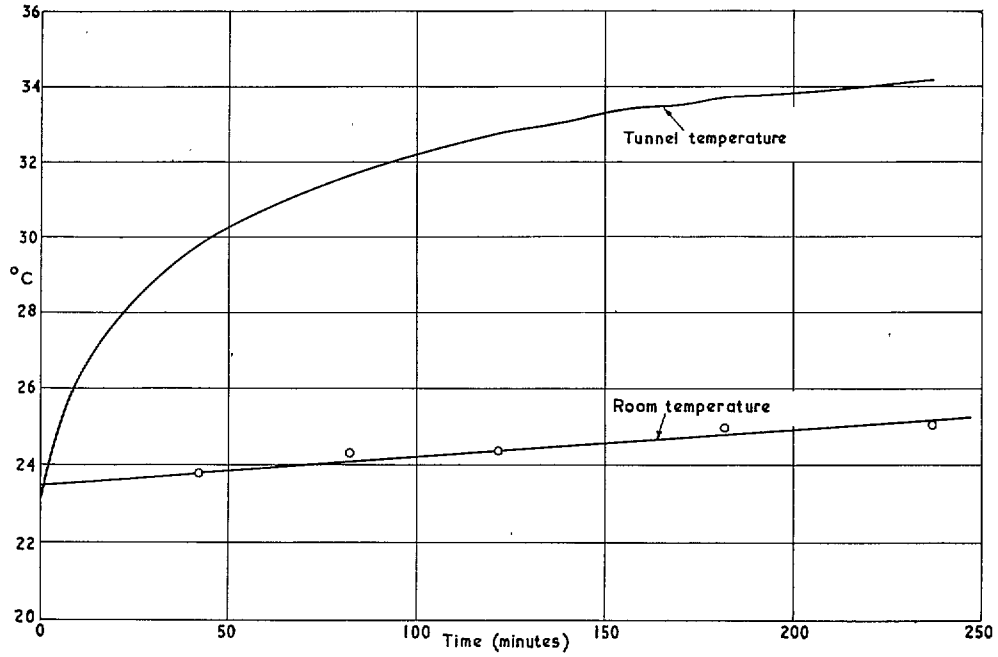

FIG. 21. Temperature drift: no tangential blowing. Reference pressure difference 4 in. alcohol: $U_1 \sim 130$ ft/sec.

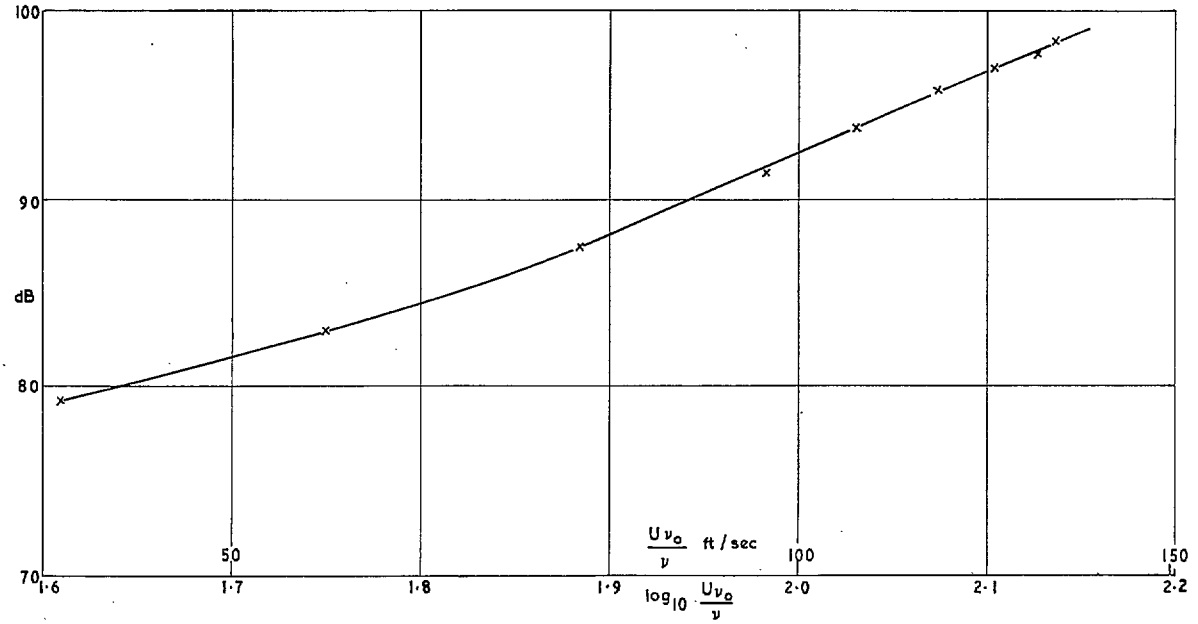

FIG. 22. Noise in settling chamber.

(92796) Wt. 67/7689 K.5 5/66 Hw.

Publications of the Aeronautical Research Council

ANNUAL TECHNICAL REPORTS OF THE AERONAUTICAL RESEARCH COUNCIL (BOUND VOLUMES)

1945 Vol. I. Aero and Hydrodynamics, Aerofoils. £6 10*s*. (£6 14*s*.)
Vol. II. Aircraft, Airscrews, Controls. £6 10*s*. (£6 14*s*.)
Vol. III. Flutter and Vibration, Instruments, Miscellaneous, Parachutes, Plates and Panels, Propulsion. £6 10*s*. (£6 14*s*.)
Vol. IV. Stability, Structures, Wind Tunnels, Wind Tunnel Technique. £6 10*s*. (£6 14*s*.)

1946 Vol. I. Accidents, Aerodynamics, Aerofoils and Hydrofoils. £8 8*s*. (£8 12*s*. 6*d*.)
Vol. II. Airscrews, Cabin Cooling, Chemical Hazards, Controls, Flames, Flutter, Helicopters, Instruments and Instrumentation, Interference, Jets, Miscellaneous, Parachutes. £8 8*s*. (£8 12*s*.)
Vol. III. Performance, Propulsion, Seaplanes, Stability, Structures, Wind Tunnels. £8 8*s*. (£8 12*s*.)

1947 Vol. I. Aerodynamics, Aerofoils, Aircraft. £8 8*s*. (£8 12*s*. 6*d*.)
Vol. II. Airscrews and Rotors, Controls, Flutter, Materials, Miscellaneous, Parachutes, Propulsion, Seaplanes, Stability, Structures, Take-off and Landing. £8 8*s*. (£8 12*s*. 6*d*.)

1948 Vol. I. Aerodynamics, Aerofoils, Aircraft, Airscrews, Controls, Flutter and Vibration, Helicopters, Instruments, Propulsion, Seaplane, Stability, Structures, Wind Tunnels. £6 10*s*. (£6 14*s*.)
Vol. II. Aerodynamics, Aerofoils, Aircraft, Airscrews, Controls, Flutter and Vibration, Helicopters, Instruments, Propulsion, Seaplane, Stability, Structures, Wind Tunnels. £5 10*s*. (£5 14*s*.)

1949 Vol. I. Aerodynamics, Aerofoils. £5 10*s*. (£5 14*s*.)
Vol. II. Aircraft, Controls, Flutter and Vibration, Helicopters, Instruments, Materials, Seaplanes, Structures, Wind Tunnels. £5 10*s*. (£5 13*s*. 6*d*.)

1950 Vol. I. Aerodynamics, Aerofoils, Aircraft. £5 12*s*. 6*d*. (£5 16*s*. 6*d*.)
Vol. II. Apparatus, Flutter and Vibration, Meteorology, Panels, Performance, Rotorcraft, Seaplanes. £4 (£4 3*s*. 6*d*.)
Vol. III. Stability and Control, Structures, Thermodynamics, Visual Aids, Wind Tunnels. £4 (£4 3*s*. 6*d*.)

1951 Vol. I. Aerodynamics, Aerofoils. £6 10*s*. (£6 14*s*.)
Vol. II. Compressors and Turbines, Flutter, Instruments, Mathematics, Ropes, Rotorcraft, Stability and Control, Structures, Wind Tunnels. £5 10*s*. (£5 14*s*.)

1952 Vol. I. Aerodynamics, Aerofoils. £8 8*s*. (£8 12*s*.)
Vol. II. Aircraft, Bodies, Compressors, Controls, Equipment, Flutter and Oscillation, Rotorcraft, Seaplanes, Structures. £5 10*s*. (£5 13*s*. 6*d*.)

1953 Vol. I. Aerodynamics, Aerofoils and Wings, Aircraft, Compressors and Turbines, Controls. £6 (£6 4*s*.)
Vol. II. Flutter and Oscillation, Gusts, Helicopters, Performance, Seaplanes, Stability, Structures, Thermodynamics, Turbulence. £5 5*s*. (£5 9*s*.)

1954 Aero and Hydrodynamics, Aerofoils, Arrester gear, Compressors and Turbines, Flutter, Materials, Performance, Rotorcraft, Stability and Control, Structures. £7 7*s*. (£7 11*s*.)

Special Volumes

Vol. I. Aero and Hydrodynamics, Aerofoils, Controls, Flutter, Kites, Parachutes, Performance, Propulsion, Stability. £6 6*s*. (£6 9*s*. 6*d*.)
Vol. II. Aero and Hydrodynamics, Aerofoils, Airscrews, Controls, Flutter, Materials, Miscellaneous, Parachutes, Propulsion, Stability, Structures. £7 7*s*. (£7 10*s*. 6*d*.)
Vol. III. Aero and Hydrodynamics, Aerofoils, Airscrews, Controls, Flutter, Kites, Miscellaneous, Parachutes, Propulsion, Seaplanes, Stability, Structures, Test Equipment. £9 9*s*. (£9 13*s*. 6*d*.)

Reviews of the Aeronautical Research Council

1949–54 5*s*. (5*s*. 6*d*.)

Index to all Reports and Memoranda published in the Annual Technical Reports

1909–1947 R. & M. 2600 (out of print)

Indexes to the Reports and Memoranda of the Aeronautical Research Council

Between Nos. 2451–2549: R. & M. No. 2550 2*s*. 6*d*. (2*s*. 9*d*.); Between Nos. 2651–2749: R. & M. No. 2750 2*s*. 6*d*. (2*s*. 9*d*.); Between Nos. 2751–2849: R. & M. No. 2850 2*s*. 6*d*. (2*s*. 9*d*.); Between Nos. 2851–2949: R. & M. No. 2950 3*s*. (3*s*. 3*d*.); Between Nos. 2951–3049: R. & M. No. 3050 3*s*. 6*d*. (3*s*. 9*d*.); Between Nos. 3051–3149: R. & M. No. 3150 3*s*. 6*d*. (3*s*. 9*d*.); Between Nos. 3151–3249: R. & M. No. 3250 3*s*. 6*d*. (3*s*. 9*d*.); Between Nos. 3251–3349: R. & M. No. 3350 3*s*. 6*d*. (3*s*. 11*d*.)

Prices in brackets include postage

Government publications can be purchased over the counter or by post from the Government Bookshops in London, Edinburgh, Cardiff, Belfast, Manchester, Birmingham and Bristol, or through any bookseller

Printed and published by
HER MAJESTY'S STATIONERY OFFICE

To be purchased from
49 High Holborn, London WC1
423 Oxford Street, London W1
13A Castle Street, Edinburgh 2
109 St. Mary Street, Cardiff
Brazennose Street, Manchester 2
50 Fairfax Street, Bristol 1
35 Smallbrook, Ringway, Birmingham 5
80 Chichester Street, Belfast 1
or through any bookseller

Printed in England

S.O. Code No. 23-3437